Nanoscale Advances

ROYAL SOCIETY OF CHEMISTRY

PAPER

View Article Online
View Journal | View Issue

Cite this: *Nanoscale Adv.*, 2023, **5**, 3463

Supramolecular Pd@methioine-EDTA-chitosan nanocomposite: an effective and recyclable bio-based and eco-friendly catalyst for the green Heck cross-coupling reaction under mild conditions†

Mohammad Dohendou, Mohammad G. Dekamin * and Danial Namaki

Supramolecular palladium(II) supported on modified chitosan by DL-methionine using an ethylenediaminetetraacetic acid linker (Pd@MET-EDTA-CS) was designed and prepared through a simple procedure. The structure of this novel supramolecular nanocomposite was characterized by different spectroscopic, microscopic and analytical techniques including FTIR, EDX, XRD, FESEM, TGA, DRS, TEM, AA, and BET. The obtained bio-based nanomaterial was successfully investigated, as a highly efficient and green heterogeneous catalyst, in the Heck cross-coupling reaction (HCR) for the synthesis of various valuable biologically active cinnamic acid ester derivatives from the corresponding aryl halides using several acrylates. Indeed, aryl halides containing I or Br survived very well under optimized conditions to afford the corresponding products compared to the substrates with Cl. The prepared Pd@MET-EDTA-CS nanocatalyst promoted the HCR in high to excellent yields and short reaction times with minimum Pd loading (0.0027 mol%) on its structure as well as without any leaching occurring during the process. The recovery of the catalyst was performed by simple filtration and the catalytic activity remained approximately constant after five runs for the model reaction.

Received 12th March 2023
Accepted 22nd May 2023

DOI: 10.1039/d3na00157a

rsc.li/nanoscale-advances

1. Introduction

To date, several cross-coupling reactions, including Heck,[1] Suzuki,[2] Sonogashira,[3] Negishi,[4] Kumada,[5] Stille,[6] and Tsuji-Trost,[7] have been introduced to create C–C bonds. These reactions have had a great impact on the decoration and design and development of organic reactions, as well as the perception of organic synthesis. Among of them, the Heck reaction has been employed broadly in a variety of synthetic protocoles, including the food and fragrance industry, agro-chemicals, fine chemicals, and for obtaining active pharmaceutical ingredients (APIs).[8,9] Mizoroki[10] and Heck[11] announced the HRC for the first time individually about 50 years ago as a Pd catalyst-mediated reaction. Indeed, this reaction has been emerged as an efficient replacement, working under mild conditions, for the Grignard reagents as well as other organic transformations to construct C=C bonds.[12–15] One of the extensive applications of the HCR is in the synthesis of cinnamic acid derivatives (CADs). Cinnamic acid (CA) is a natural aromatic carboxylic acid, which is found in plants and honey.[16] Scientific research has demonstrated that CA exhibits biological and chemical properties, including antioxidant, antimicrobial, anti-inflammatory,[17,18] anti-cancer,[19,20] neuroprotective,[21] and antidiabetic,[22,23] as well as acting as a UV protector in cosmetics,[24] precursor of shikimic acid, an important intermediate in the pharmaceutical industry[25] and precursor of fragrance materials.[26] Although there are natural sources of CADs, several chemical and biochemical methodologies have been reported for their synthesis, including the Claisen–Schmidt condensation,[27] Perkin reaction,[28] Knoevenagel condensation promoted by tetraalkylammonium halides[29] or accelerated by MW irradiation,[30] the application of phosphorous oxychloride,[31] or DDQ under ultrasonic conditions,[32] biocatalytic synthesis,[33,34] and HCR.[1,27,35,36] Among these procedures, green HCR catalyzed by biopolymeric-based catalytic systems has been recieved graet attention recently.[37–39] Definitely, the essential part of the HCR is its catalytic system. In recent years, several methods have been reported for this transformation.[36,40–42] Although homogeneous catalysts have shown high activities, various drawbacks, including the necessity to add toxic ligands such as PPh_3, contamination of the final products by Pd, the troublesome and laborious recycling processes, and the high price of Pd, have led to the design of alternative heterogeneous catalysts in both laboratory and industrial research and development.[42–52] Therefore, it is vital to design and develop novel green catalytic systems according to green chemistry

Pharmaceutical and Heterocyclic Compounds Research Laboratory, Department of Chemistry, Iran University of Science and Technology, Tehran 16846-13114, Iran. E-mail: mdekamin@iust.ac.ir

† Electronic supplementary information (ESI) available. See DOI: https://doi.org/10.1039/d3na00157a

(GC) principles for promoting the HCR. In this regard, different catalysts have been introduced to facilitate the recycling and reuse of the catalysts and for purification of the desired products without any transition metal contamination, as well as avoiding the use of toxic ligands and reducing the consumption of precious Pd, which address the drawbacks of the previous protocols.[48,53–63] One of the emerging improvements in the design and preparation of heterogeneous functionalized catalytic systems is grafting appropriate moieties onto the surface of renewable and biodegradable naturally occurring biopolymeric materials. This approach demostrates several advantages, including its ecologically benign nature, use of abundant supports, easy recyclability, and proper biodegrability, which all address the aims of green and sustainable chemistry in the 21st century.[36,64–74] Because of the presence of both free NH_2 and OH functional groups in the structure of chitin and especially its deacetylated derivative, chitosan,[71] the application of these biodegradable and biocompatible materials have received extensive consideration recently in sustainable chemistry as excellent supports for catalytic systems.[75–88] Chitosan now plays a vital role in different fields, including medicine, drug delivery, food packaging, cosmetics, water treatment, membranes, fuel cells, hydrogels, adhesives, and surface conditioners.[89–97] Indeed, the NH_2 groups with high chelating ability as well as the proper geometry of neighboring OH groups in the chitosan scaffold along with its insolubility in the majority of organic solvents and water make it the best candidate for using in the preparation of robust supramolecular heterogeneous catalysts by both academia and the chemical industry, especially in the pharmaceutical sector. Therefore, pristine chitosan and its modified structures have received considerable attention in various catalytic systems for different organic transformations.[40,98] In this context, chitosan surface modifications by appropriate moieties having proper other functional groups provide new more efficient and well-tuned supports, compared to the previous ones, for achieving the desired catalytic chemical reactions.[99–101] On the other hand, ethylenediaminetetraacetic acid (EDTA) has been applied as a supramolecular chelating and ion exchange agent for several metal ions in many preceding publications.[102–105] EDTA has also outstanding ability to act as a low-cost and non-toxic cross-linker for creating strong bonds with organic nucleophilic functional groups.[106–108] Hence, EDTA has been recently used as a linker to afford several nanocatalytic systems, such as chitosan-EDTA for Knoevenagel condensation reaction,[109] chitosan-EDTA-cellulose network for Hantzsch esters and 4*H*-pyrans synthesis,[80,84] L-asparagine-EDTA-amide silica-coated MNPs for 3,4-dihydropyrimidin-2(1*H*)-ones synthesis,[110] and diamide-diacid-bridged PMO for the cascade oxidation of benzyl alcohols/Knoevenagel condensation,[111] and Pd@ASP-EDTA-CS for HCR.[112] Moreover, methionine is one of the nine essential amino acids in the human body, which is provided by foods. Methionine is the only sulfur-containing essential amino acid that is necessary for growth and tissue repair, increasing the quality and elasticity of skin and hair, and strengthening the nails. It also plays a significant role in many biological actions, such as methylation and antioxidant properties, as well as its usage in the synthesis of proteins.[113–116] Infact, the sulfur element in the methionine helps cells to defend against pollutants, decreases cell aging, and is crucial for the absorption and bioavailability of selenium and zinc. Additionally, methionine chelates heavy metals, such as Pb and Hg, aiding their elimination.[117] Consequently, based on green, economical, and well-being considerations, it would be desirable to develop simple and operative procedures for the HCR by using heterogeneous Pd catalytic systems using chitosan, EDTA, and methionine.[64,65,67,118–123] To the best of our knowledge and in continuation of our previous research,[112] we herein for the first time report the preparation and characterization of a novel supramolecular Pd(II) supported on a modified naturally occurring chitosan backbone (Pd@MET-EDTA-CS, **1**). The novel Pd@MET-EDTA-CS nanocatalyst was prepared by modifying chitosan biopolymeric chains by DL-methionine using EDTA dianhydride (EDTADA), as a linker with proper reactivity, and by subsequent chelating of $PdCl_2$ onto its surface (Scheme 1). The Pd@MET-EDTA-CS nanocomposite **1** with an ultralow Pd loading (0.286 wt%) was used in the HCR, which promotes the reaction to occur at a lower temperature and shorter reaction times to afford the corresponding CADs in good to excellent yields under mild conditions.

2. Experimental

2.1. General information

Chitosan (MW = 190–300 kDa, medium molecular weight, 75–85% deacetylation degree) was purchased from across. EDTA (MW = 292.24 g mol^{-1}) was supplied by Merck. DL-methionine (MW = 149.21 g mol^{-1}) was purchased from an approved local supplier. Acrylic acid, methyl acrylate, ethyl acrylate, butyl acrylate, aryl halides, and $PdCl_2$ were purchased from various international chemical companies, comprising Mreck, Sigma-Aldrich and Samchun. The analytical TLC experiments were performed using Merck Kieselgel 60 F-254 Al-plates followed by visualization under UV light and iodine vapor. To identify the functional groups of the samples, FTIR spectroscopy (Perkin Elmer 1720-X) was utilized in the range of 600–4000 cm^{-1} using KBr disks. An Electrothermal 9100 A apparatus was employed to measure the melting points of the products. X-Ray diffraction and energy-dispersive X-ray spectroscopy were performed for analysis of the catalyst on a XRD Bruker D8 system (Germany) and EDX Bruker system (Germany), respectively. The morphologies of the fresh and recycled catalyst were examined by FESEM (KYKY EM8000) and FESEM (TESCAN VEGA3), respectively. The related elements of the fresh catalyst were observed by FESEM mapping. The TGA curves of the catalyst **1** were recorded on a Bahr STA 504 instrument, while a Micromeritics A 2020 device was used for the Brunauer–Emmett–Teller (BET) test. The TEM images were taken using an EM 208S Philips microscope (operated at 100 kV). The mol% of the catalyst **1** was calculated based on the result of the Pd content in the nanocatalyst, which was determined by atomic absorption spectroscopy (AA, GBC 932 plus) (Table S4, ESI†). The ^1H NMR

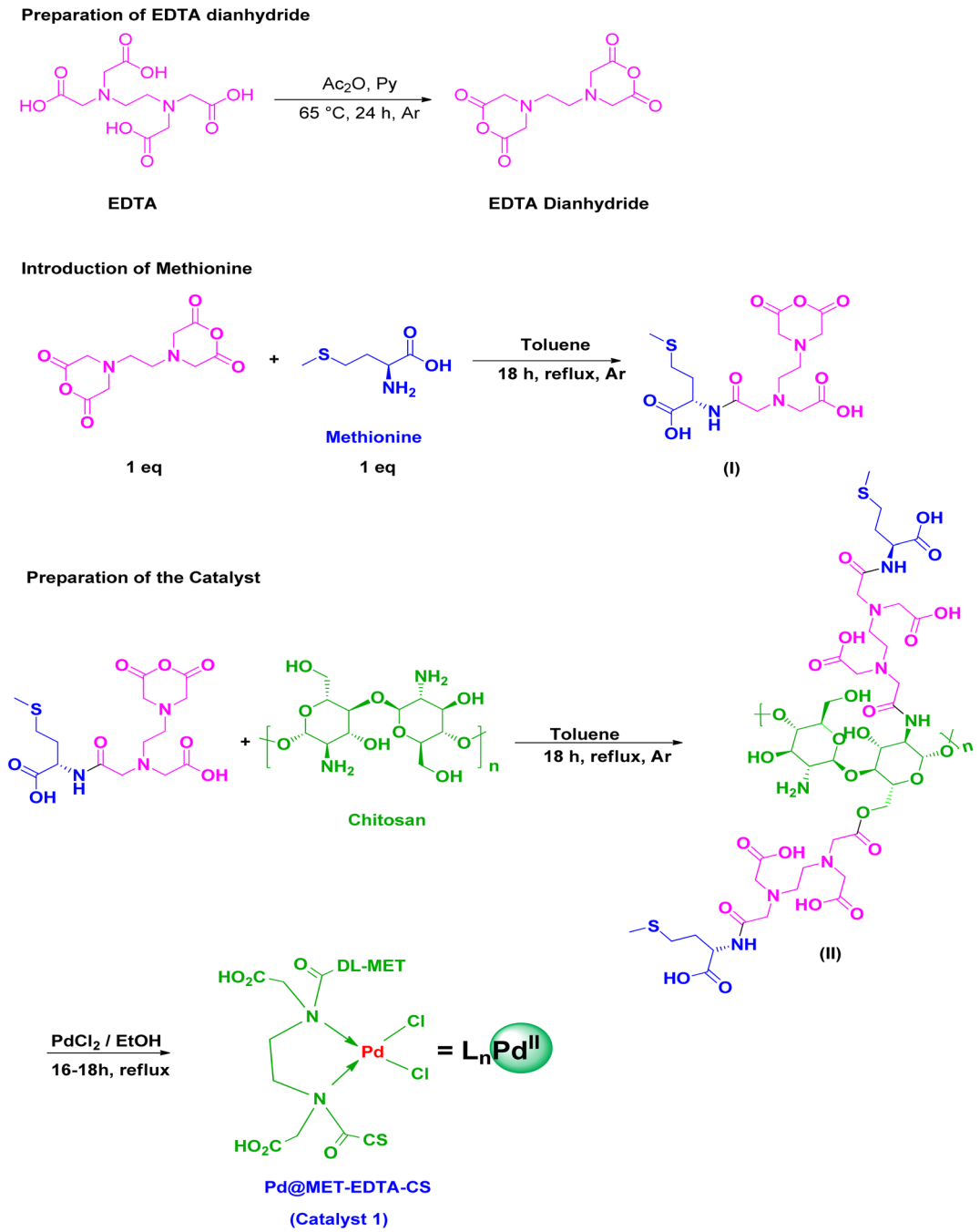

Scheme 1 Schematic representation for the preparation of the Pd@MET-EDTA-CS nanocatalyst (1).

spectra of the isolated products were recorded at 500 MHz using a Varian-INOVA spectrometer in DMSO-d_6 at ambient temperature.

2.2. General procedure for the preparation of EDTA dianhydride (EDTADA)

EDTA (10.0 g, 34.0 mmol), pyridine (16 mL), and acetic anhydride (14.0 mL) were charged into a 100 mL round-bottom flask equipped with a condenser and a magnetic stirrer. The reaction was mixed and stirred at 65–70 °C for 24 h under an Ar atmosphere. After completion of the reaction, the suspension was filtered and the crude product was washed with acetic anhydride (5.0 mL) and dry Et_2O (10.0 mL) under an atmosphere of Ar to afford a white powder. The final product was dried by using a rotary evaporator under vacuum at 40–50 °C until a fine and dry white powder was obtained (yield 91–93%, m.p.: 189–191 °C; Scheme 1).[124,125]

2.3. Preparation of the DL-methionine-EDTA monoanhydride (MET-MAEDTA, intermediate I)

The as-prepared EDTADA (0.256 g, 1.0 mmol) was charged into a two-neck round-bottom flask equipped with a reflux

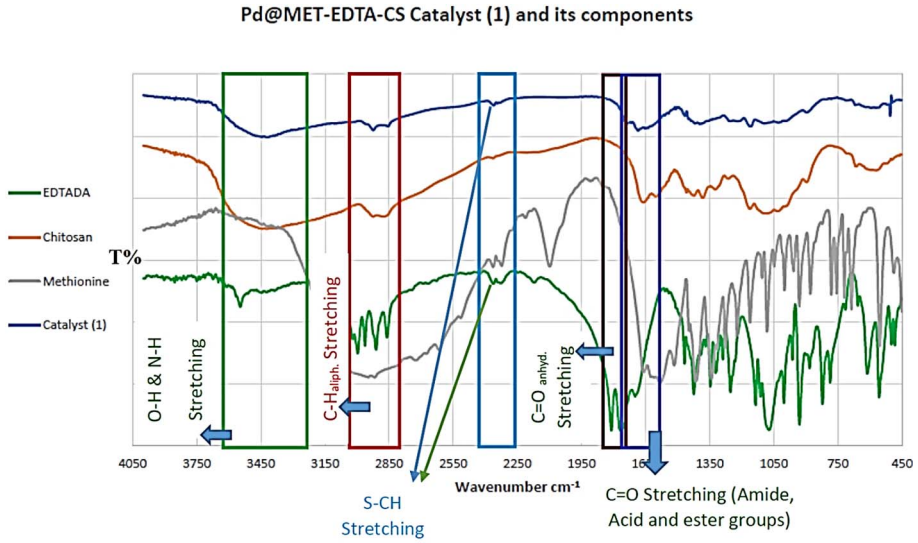

Fig. 1 FTIR spectra of the Pd@MET-EDTA-CS catalyst (**1**) and its components.

condenser and a magnet bar. Then, 3.0 mL of dry toluene was added under an Ar atmosphere. After that, DL-methionine solution (0.149 g, 1.0 mmol in 2.0 mL toluene) was gradually added over 60 min to control the selective reaction with one anhydride functional group of the EDTADA. Finally, the mixture was stirred and heated under reflux conditions and an Ar atmosphere for 18 h. The desired intermediate (**I**) was filtered and dried under vacuum at 60 °C by using a rotary evaporator to afford a creamy white powder (0.394 g, yield = 93%).[84,126]

2.4. Preparation of DL-methionine-ETDA grafted on chitosan (intermediate II)

MET-MAEDTA (**I**, 0.16 g) and chitosan (0.32 g) were charged into a double-neck round-bottom flask containing dry toluene (10 mL). After that, the mixture was stirred and heated at 60–70 °C under an Ar atmosphere for 18 h. After completion of the reaction, the mixture was cooled down to ambient temperature and the suspension was filtered and dried in a vacuum oven at 70 °C to afford the desired intermediate (**II**) (0.45 g, 94%, Scheme 1).

2.5. Preparation of the Pd@MET-EDTA-CS catalyst (1)

$PdCl_2$ (20.0 mg) was added to the suspension of intermediate (**II**) (400 mg in 3.0 mL EtOH) and the obtained mixture was refluxed for 18 h. After cooling the reaction mixture to ambient temperature, the prepared catalyst (**1**) was filtered and washed under vacuum with EtOH (96%, 2 mL) and then dried in an oven at 70 °C to afford the desired catalyst **1** (0.35 g, Scheme 1).

2.6. General procedure for the synthesis of cinnamic acid derivatives 5a–l in the HCR catalyzed by the Pd@MET-EDTA-CS catalyst (1)

A mixture of aryl halide (**2a–e**, 2.0 mmol), active alkenes (**3a–d**, 3.0 mmol), potassium carbonate (2.0 mmol), and catalyst **1** (2.0 mg, 0.0027 mol%) were added into a double-neck round-bottom flask containing a proper solvent, CH_3CN or DMF (3.0 mL), and heated under an Ar atmosphere at 80–90 °C for an appropriate amount of time as indicated in Table 2. At the endpoint of the reaction, as monitored by TLC [eluent : *n*-hexane : EtOAc: 5 : 1], the mixture was cooled down to ambient temperature, and the catalyst was filtered by vacuum and washed by 5.0 mL water to dissolve any unreacted salts. Then, it was washed with EtOH (96%, 2 mL) and dried to be used in the next reaction cycles. The solvent of the filtrate was recovered under reduced pressure. After that, water (3.0 mL) and $CHCl_3$ (3.0 mL) were added to the residue followed by stirring for 30 min. After settling for 0.5 h, the two layers were decanted, to separate out the undesired salts and materials. Afterward, the water content of the organic layer was removed by using dry Na_2SO_4. Next, the organic phase was evaporated on a rotary evaporator to afford the crude products. Ultimately, the crude products were recrystallized from EtOH to obtain the pure corresponding CADs **4a–l**.

2.7. Spectral data of the selected products methyl cinnamate (4b)

White crystals, m.p. = 34–38 °C; FTIR (KBr, cm^{-1}) ν = 3450, 3400, 2920, 2855, 2368, 1742, 1681, 1650, 1557,1453, 1218, 1156, 1100, 898, 700, 665; ^1H NMR (500 MHz, DMSO-d_6) δ (ppm) = 3.71 (s, 3H, OCH_3), 6.59 (1H, d, J = 16.0 Hz, MeOCCH=), 7.40 (2H, m, Ar–H), 7.64 (3H, m, Ar–H), 7.69 (1H, d, J = 16.0 Hz, ArCH=) (Fig. S11 and S12†).

3. Results and discussion

3.1. Characterization of the Pd@MET-EDTA-CS catalyst (1)

The inclusive processes for the synthesis of Pd@METH-EDTA-CS (catalyst **1**) is illustrated in Scheme 1. The catalyst was characterized by using various spectroscopic, microscopic, and analytical techniques including Fourier-transform infrared (FTIR) spectroscopy, energy-dispersive X-ray (EDX)

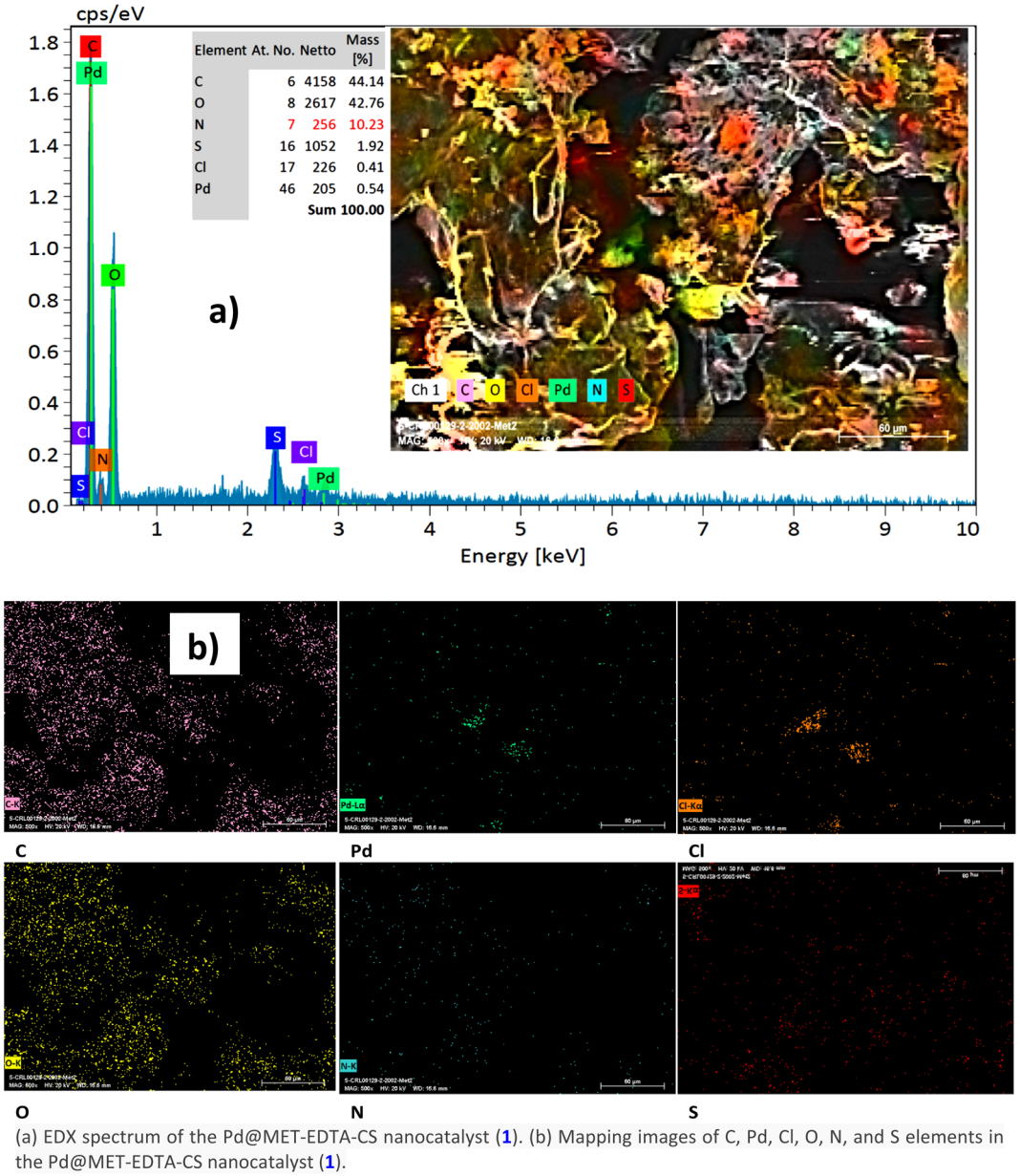

(a) EDX spectrum of the Pd@MET-EDTA-CS nanocatalyst (1). (b) Mapping images of C, Pd, Cl, O, N, and S elements in the Pd@MET-EDTA-CS nanocatalyst (1).

Fig. 2 (a) EDX spectrum of the Pd@MET-EDTA-CS nanocatalyst (1). (b) Mapping images of C, Pd, Cl, O, N, and S elements in the Pd@MET-EDTA-CS nanocatalyst (1).

spectroscopy, field-emission scanning electron microscopy (FESEM), X-ray powder diffraction (XRD), thermogravimetric analysis (TGA), transmission electron microscopy (TEM), atomic absorption spectroscopy (AAS), Brunauer–Emmett–Teller (BET) surface area analysis, and differential reflectance spectroscopy (DRS).

3.1.1. Fourier-transform infrared (FTIR) analysis. To determine the functional groups and structure of EDTADA (green), chitosan (orange), DL-methionine (gray) and the Pd@MET-EDTA-CS catalyst **1** (blue), FTIR spectroscopy was employed. The results are exhibited in the overlay spectra in Fig. 1. The detected bands at 3400–3600 cm^{-1} are related to the hydroxyl and amine groups, while the asymmetric and symmetric stretching vibrations of C=O groups in EDTA dianhydride are displayed at 1809 and 1756 cm^{-1}, respectively. These bands are displaced by the formed C=O groups of the amide, acid, and ester during the preparation of the catalyst **1** at 1650, 1681, and 1730 cm^{-1}, respectively. The sp^3 C–H vibration bands are observed at 2900–3000 cm^{-1}, while the signals at 1200–1400 cm^{-1} are assigned to the bending of –NH groups. The C–O stretching bands are located at about 1100 cm^{-1}, while the band at 665–700 cm^{-1} is related to the presence of C–S–C.

3.1.2. Energy-dispersive X-ray (EDX) spectroscopy analysis. The chemical composition and surface elemental analysis of the Pd@MET-EDTA-CS (**1**) was carried out by means of energy-dispersive EDX. The EDX spectrum of catalyst and the

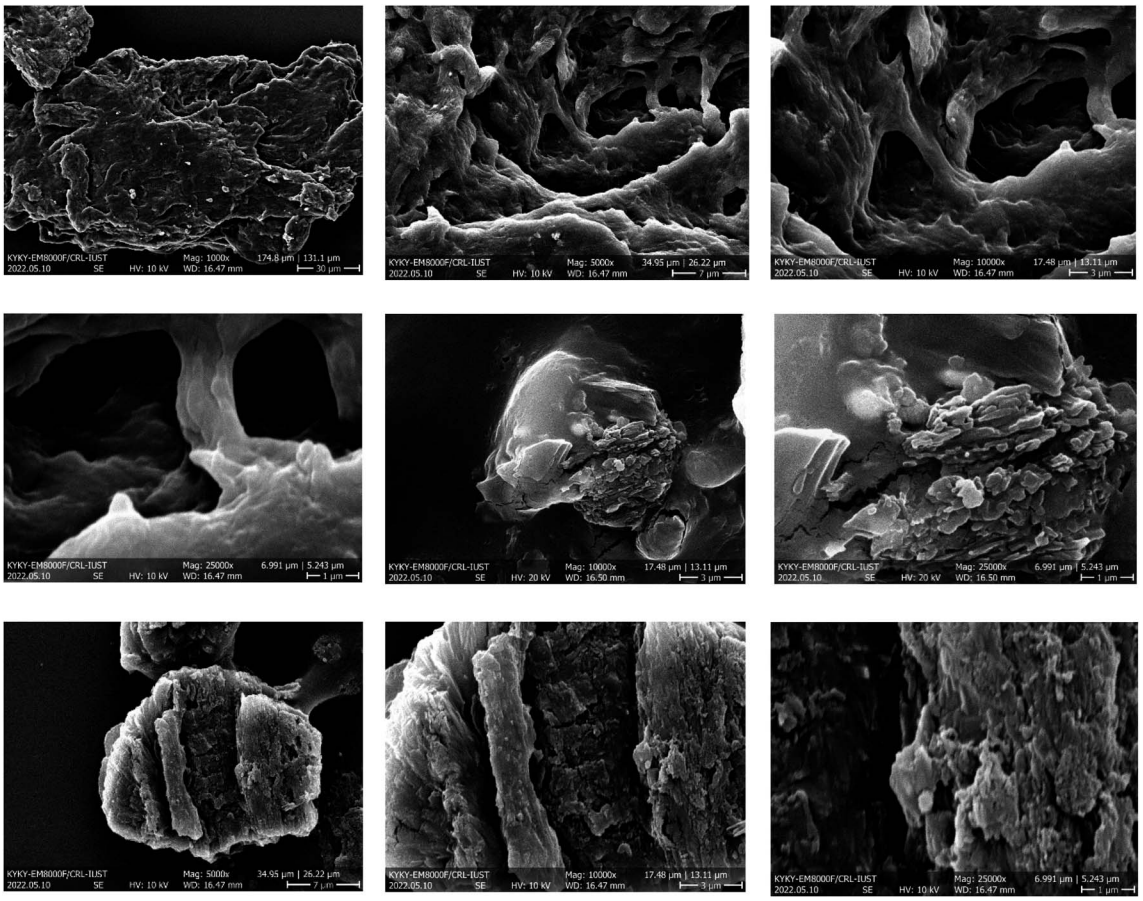

Fig. 3 FESEM images of the Pd@MET-EDTA-CS nanocatalyst (**1**).

mapping images of the relevant elements are illustrated in Fig. 2a and b, respectively. Indeed, the EDX analysis exhibited well-defined peaks related to C, O, N, S, Cl, and Pd in the structure of the Pd@MET-EDTA-CS (**1**), with percentages of 44.14%, 42.76%, 10.23%, 1.92%, 0.41%, and 0.54%, respectively.

3.1.3. Field-emission scanning electron microscopy (FESEM) analysis. The morphology and texture of the Pd@MET-EDTA-CS nanocomposite (**1**) were specified by FESEM analysis and the acquired images are presented in Fig. 3. According to the FESEM images, the size and surface morphology of the catalyst could be well observed and demonstrated that the particles had a special layered structure with defined pores and without significant agglomeration.

3.1.4. Differential reflectance spectroscopy (DRS) of the catalyst 1. The comparison between the DRS of the catalyst (**1**) and its components demonstrated that the structure of catalyst consisted of bands and groups, which were also found in the precursors (Fig. 4a). For more clarification, by setting the excel adjustments on the secondary axis of catalyst curve, more recognizable points of the combination could be implied (Fig. 4b).

3.1.5. X-Ray diffraction (XRD) analysis of the catalyst 1. The XRD pattern of the Pd@MET-EDTA-CS (**1**) is presented in Fig. 5. The detected peaks were compared with the standard reference patterns of EDTA (card no. JCPDS, 00-033-1672), chitosan (card no. JCPDS, 00-039-1834), DL-methionine (card no. JCPDS, 00-005-0311), and $PdCl_2$ (card no. JCPDS, 00-001-0228). The sharp peaks in the pattern showed the presence of crystalline sections in the structure of the catalyst **1**, as well as a combination of several peaks after grafting DL-methionine onto the chitosan scaffold by the EDTA linker followed by the chelation of Pd(II).

3.1.6. Thermogravimetric analysis (TGA) and BET of the catalyst 1. The thermal stability of the Pd@MET-EDTA-CS nanocomposite (**1**) was examined under air in the temperature range of 50–1000 °C (Fig. 6a–c). The degradation percentage in the defined temperature range for the catalyst was about 3 wt% below 100 °C, and 35 wt% in the range of 220–320 °C, which represented the removal of water or other organic solvents and the degradation of DL-methionine moieties, respectively. The nanocomposite **1** showed another mass loss (about 20 wt%) over the temperature range of 320–450 °C, which could be attributed to the decomposition of the remaining EDTA and chitosan moieties in the catalyst structure. A further mass loss in the range of 450–650 °C (about 30 wt%) was noted that is related to a complete degradation of the chitosan backbone catalyzed by Pd(II) species.[127] The total decrease in the weight of the catalyst reached about 88%, which obviously proved the effect of the

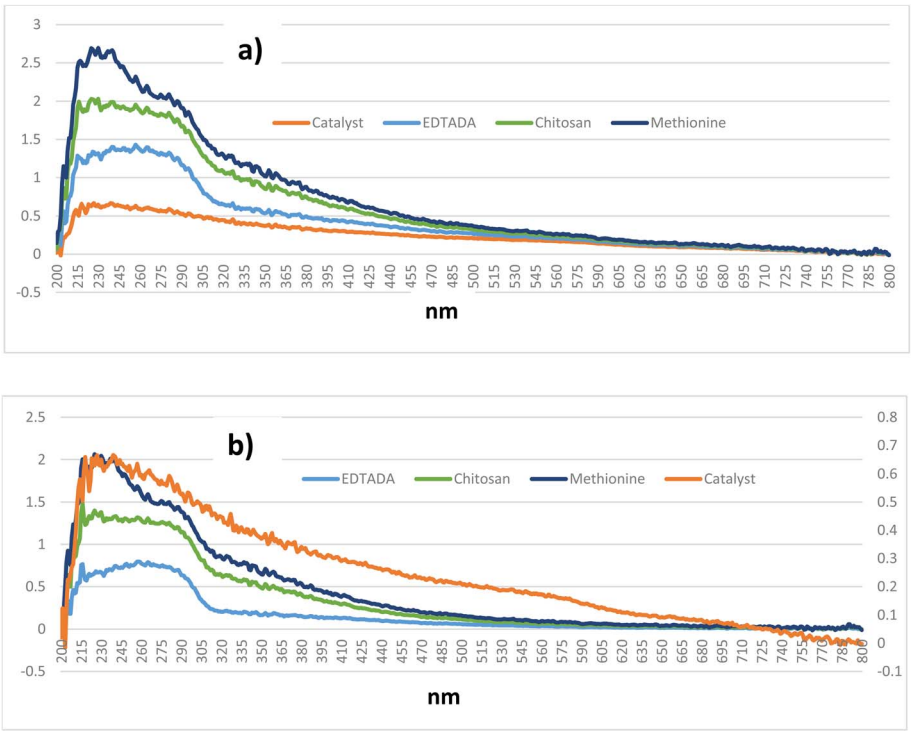

(a) DRS of the Pd@MET-EDTA-CS catalyst (1) and its components. (b) Intensified DRS of the Pd@MET-EDTA-CS catalyst (1).

Fig. 4 (a) DRS of the Pd@MET-EDTA-CS catalyst (**1**) and its components. (b) Intensified DRS of the Pd@MET-EDTA-CS catalyst (**1**).

organic units grafted onto the surface of the chitosan polymeric chains. The stability of the catalyst was up to about 270 °C, as can be seen in the differential TGA curve (**b**). These results are also indicated that EDTA and DL-methionine had been successfully grafted onto the chitosan polymeric surface. In comparison to the pristine chitosan, the effect of chelated Pd nanoparticles on the biopolymeric support caused an increase in the thermal stability of the nanocatalyst. Moreover, the differential DTA curve (**c**) illustrated different exothermic and endothermic points at about 460 °C and 630 °C (melting range), respectively, and then the slope remained approximately constant to 800 °C.[128]

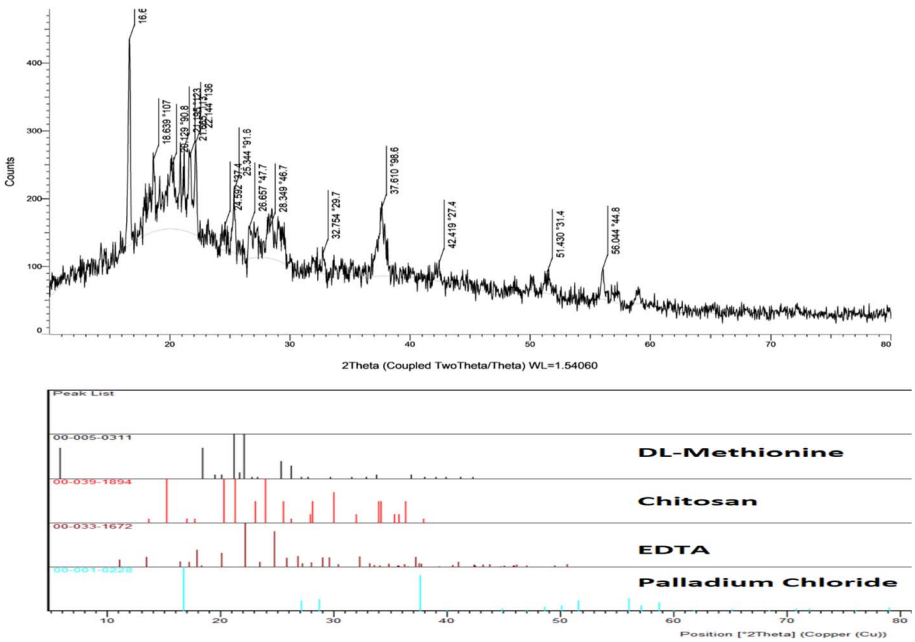

Fig. 5 XRD pattern of the Pd@MET-EDTA-CS catalyst (**1**).

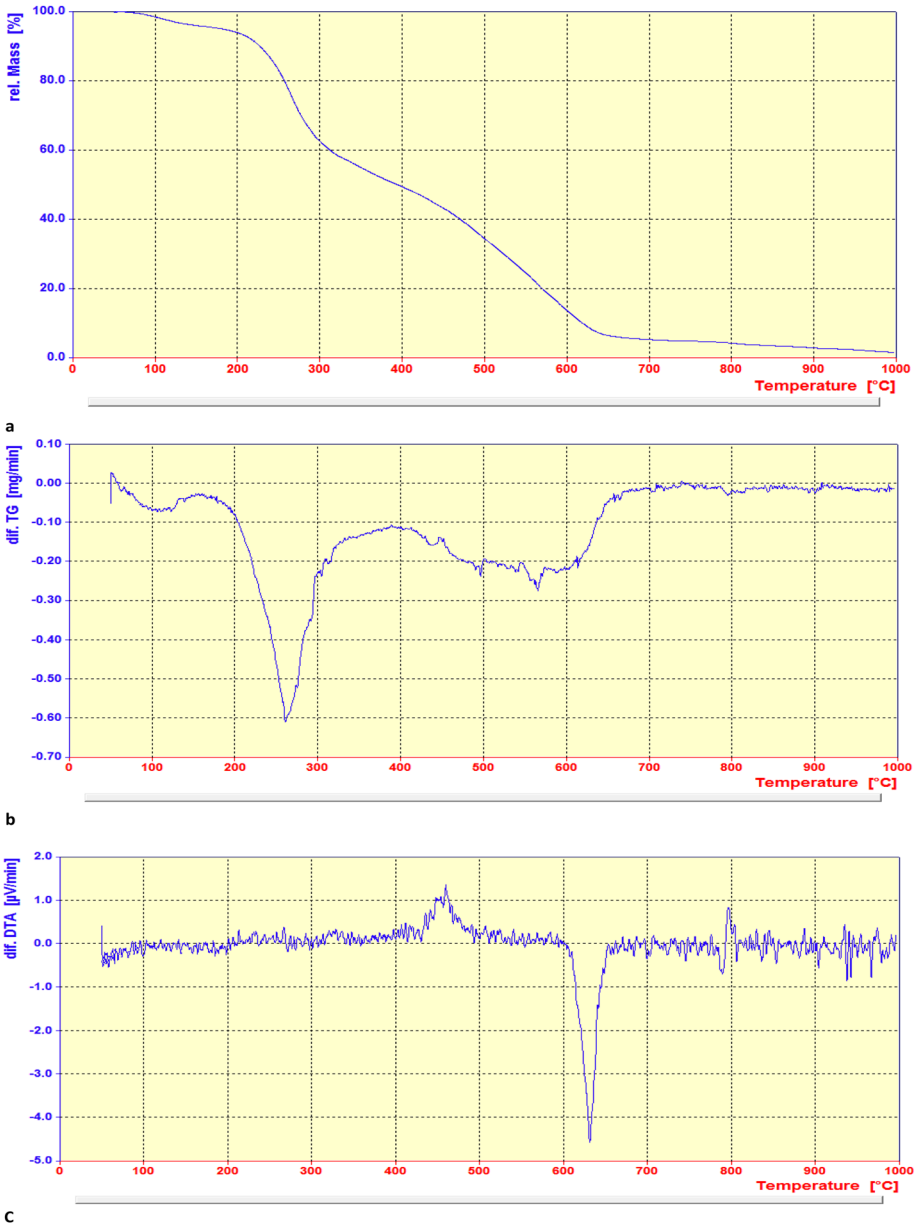

Fig. 6 (a) TGA, (b) differential TGA and (c) differential DTA curves of the Pd@MET-EDTA-CS catalyst (**1**).

In addition, the porosity of the Pd@MET-EDTA-CS (**1**) was investigated *via* the physisorption of N_2 at 77 K (Fig. 7a and b). The illustrative diagram of the catalyst for this displayed a type **III** nitrogen gas sorption isotherm, which indicated that there were plentiful microspores in the supramolecular biopolymeric-based catalyst **1**. These results proved that the specific surface area of the catalyst **1** was about 25.4 $m^2\ g^{-1}$. The BJH adsorption cumulative volume of pores with widths between 17.0 Å and 3000.0 Å was 0.026473 $cm^3\ g^{-1}$; while the BJH adsorption average pore width (4 V/A) was 50.7 Å; the BJH desorption average pore width (4 V/A) was 57.5 Å, and the adsorption average pore width (4 V/A by BET) was 37.7 Å.

3.1.7. Transmission electron microscopy (TEM) analysis. The morphology and the size distribution of the Pd@MET-EDTA-CS catalyst (**1**) were also studied by using TEM. The TEM images of the fresh catalyst **1** are shown in Fig. 8. In these images, apart from the Pd nanoparticles (well-dispersed spots with average diameters smaller than 5 nm), the polymeric sheets of modified CS could also be detected. The TEM analysis showed the special morphology of the nanocomposite **1** and the presence of uniform spherical Pd nanoparticles distributed on the composite.

3.2. Optimization of the conditions in the HCR reaction using the Pd@MET-EDTA-CS catalyst (1)

In this part of our research, the activity of the as-prepared catalyst **1** was assessed in the synthesis of cinnamic acid derivatives (CADs, **4**) through the Heck cross-coupling reaction between different halobenzenes and various active alkenes. For

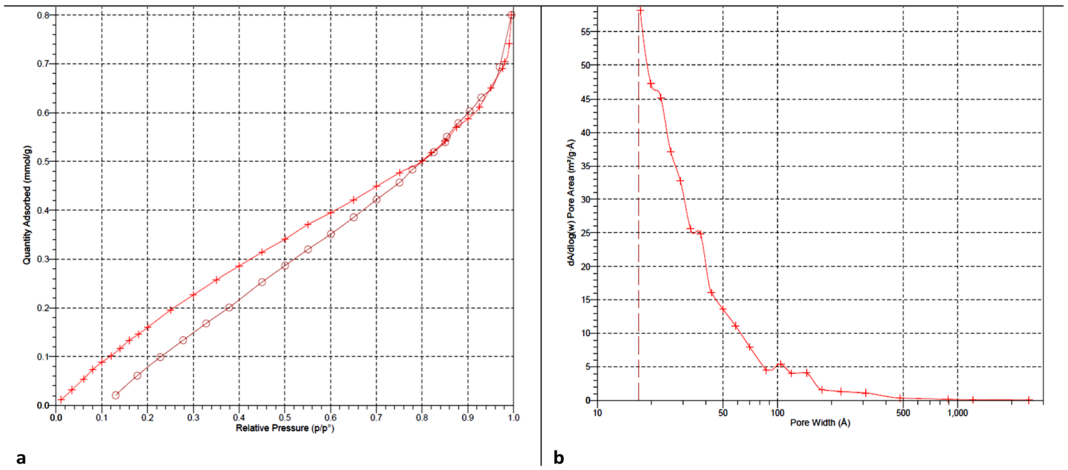

Fig. 7 (a) N_2 adsorption–desorption isotherm of the Pd@MET-EDTA-CS catalyst (**1**), and (b) its pore width.

this reason, the reaction conditions were optimized by investigating certain mixtures of iodobenzene (**2a**, 2.0 mmol), methyl acrylate (**3b**, 3.0 mmol), and K_2CO_3 (2.0 mmol) as the model reaction in the proper solvents. In a systematic screening, the reaction conditions were investigated accurately by considering several crucial variables, including the catalyst loading, reaction

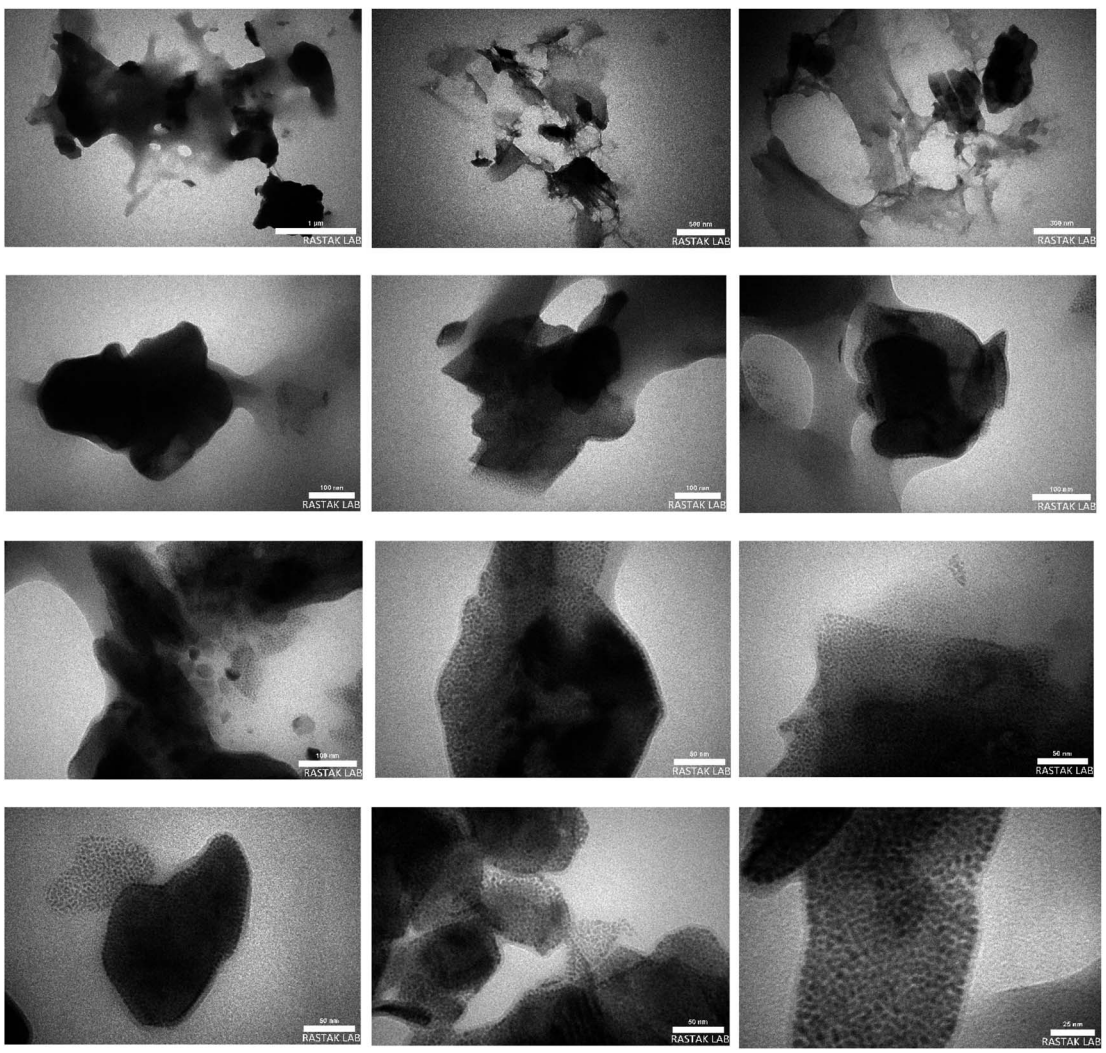

Fig. 8 TEM images of the Pd@MET-EDTA-CS nanocatalyst (**1**).

Table 1 Optimization of the conditions for the HCR in the model reaction of iodobenzene (**2a**) and methyl acrylate (**3b**) to afford methyl cinnamate (**4b**) in the presence of the Pd@MET-EDTA-CS catalyst (**1**, 0.0027 mol%)[a]

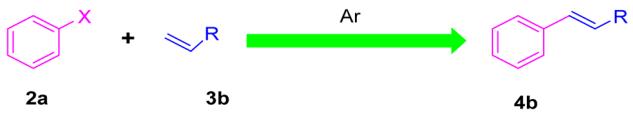

Entry	Catalyst	Base	Solvent	Temp. (°C)	Time (h)	Yield[b] (%)
1	—	K_2CO_3	DMF	r.t	48	N.R
2	—	K_2CO_3	DMF	Reflux	48	N.R
3	Pd@MET-ETDA-CS	—	DMF	Reflux	48	N.R
4	Pd@MET-ETDA-CS	—	ACN	Reflux	48	N.R
5	Pd@MET-ETDA-CS	—	Solvent-free	80	24	Trace
6	Pd@MET-ETDA-CS	K_2CO_3	**DMF**	**90**	**12–16**	**80–95**
7	Pd@MET-ETDA-CS	K_2CO_3	**ACN**	**80**	**13–19**	**80–95**
8	Pd@MET-ETDA-CS	K_2CO_3	Toluene	105	36	Trace
9	Pd@MET-ETDA-CS	K_2CO_3	H_2O	105	36	Trace
10	MET-ETDA	K_2CO_3	DMF	130	36	N.R
11	MET-ETDA-CS	K_2CO_3	DMF	130	36	N.R
12	MET-ETDA	K_2CO_3	ACN	80	36	N.R
13	MET-ETDA-CS	K_2CO_3	ACN	80	36	N.R
14	DL-Methionine	K_2CO_3	DMF	130	36	N.R
15	EDTA	K_2CO_3	DMF	130	36	N.R

[a] Reaction conditions: aryl halide (**3a**, 2.0 mmol), alkene (**4b**, 3.0 mmol), K_2CO_3 (2.0 mmol), Pd@MET-EDTA-CS (**1**) (2.0 mg, 0.0027 mol%), and solvent (3.0 mL), under an Ar atmosphere. [b] Isolated yields.

time, solvent, and reaction temperature, as given in Table 1. For the first test, in the absence of any catalyst, the progress of the model reaction even after a long reaction time at r.t. or under reflux conditions was not detected (entries 1 and 2). In addition, there was no detectable yield for the model reaction in the presence of the Pd@MET-EDTA-CS catalyst (**1**) without using the K_2CO_3 base (entries 3 and 4). A trace amount of the favored product, methyl cinnamate (**4b**), was obtained by simultaneous using of the catalyst (**1**, 0.0027 mol%) and K_2CO_3 under solvent-free conditions (entry 5). By utilizing both the catalyst and base in proper solvents, including DMF or CH_3CN, the best yields for the desired product were obtained (entries 6 and 7). On the other hand, the model reaction in toluene or water afforded only a trace amount of the desired product (entries 8 and 9). Moreover, the model reactions in the presence of EDTA, MET-EDTA, the polymeric support (MET-EDTA-CS), and DL-

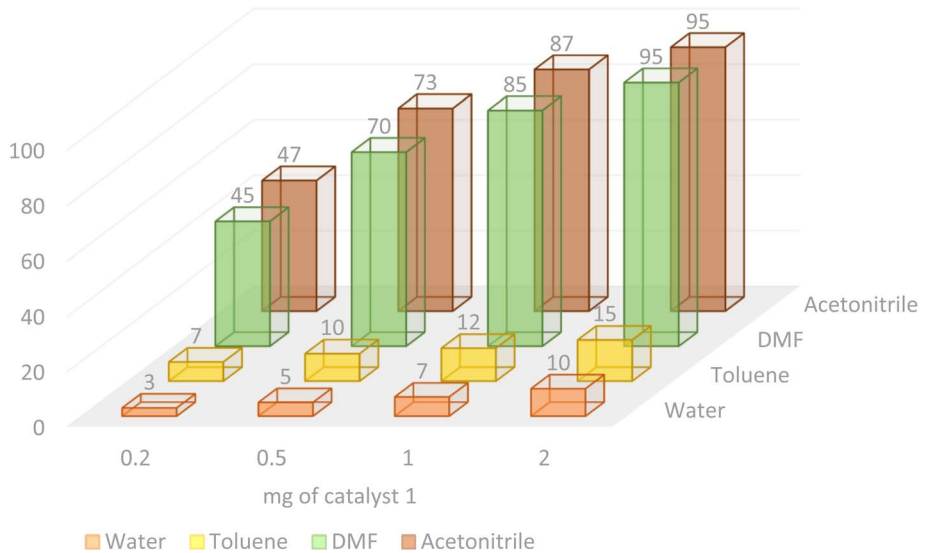

Fig. 9 Investigation of the optimized loading of the Pd@MET-EDTA-CS catalyst (**1**) in different solvents for the HCR to afford **4b**.

Table 2 Synthesis of different derivatives of cinnamic acid (4a–l) through the HCR catalyzed by the Pd@MET-EDTA-CS catalyst (1) under the optimized conditions[a]

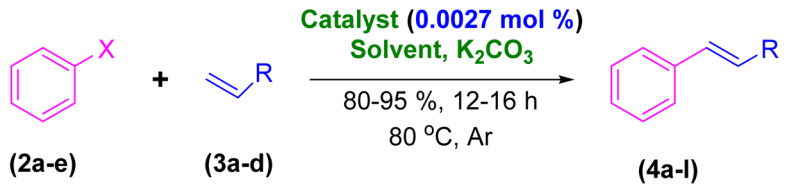

Entry	Ar-X	Alkene	Product	Time (h)	Temp. (°C)	Yield[b] (%)	TON	TOF (h^{-1})	m.p. (°C)	m.p. (°C) (Lit.)
1	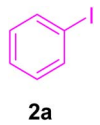 2a	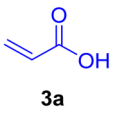 3a	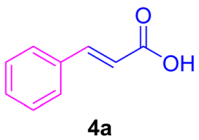 4a	12	80	90	33 330	2778	131–132	133 (ref. 135)
2	 2b	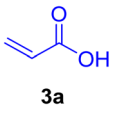 3a	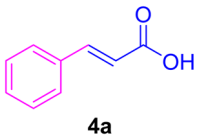 4a	14	80	80	29 630	2116	131–132	133
3	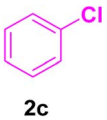 2c	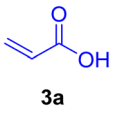 3a	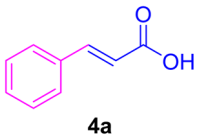 4a	40	80	20	7407	185	131–132	133
4	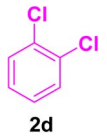 2d	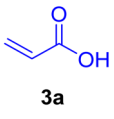 3a	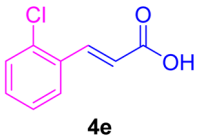 4e	48	80	Trace	NA	NA	—	212
5	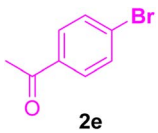 2e	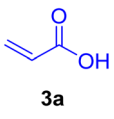 3a	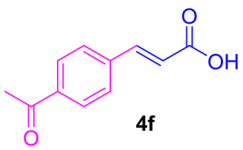 4f	48	80	Trace	NA	NA	—	224–226 (ref. 136)
6	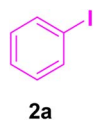 2a	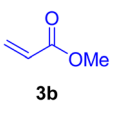 3b	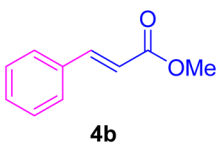 4b	13	80	95	35 185	2706	33–35	34–38 (ref. 137)
7	 2b	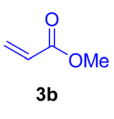 3b	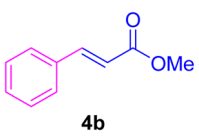 4b	15	80	85	31 481	2099	33–35	34–38
8	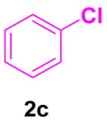 2c	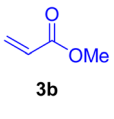 3b	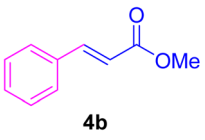 4b	36	80	20	7407	206	—	34–38
9	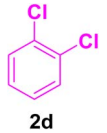 2d	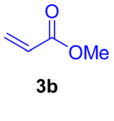 3b	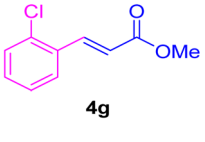 4g	48	80	Trace	NA	NA	—	34–38

Table 2 (*Contd.*)

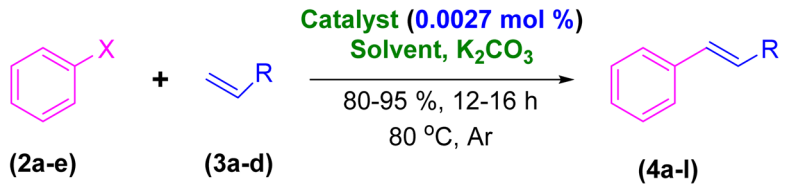

Entry	Ar-X	Alkene	Product	Time (h)	Temp. (°C)	Yield[b] (%)	TON	TOF (h^{-1})	m.p. (°C)	m.p. (°C) (Lit.)
10	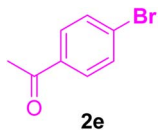 2e	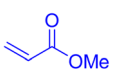 3b	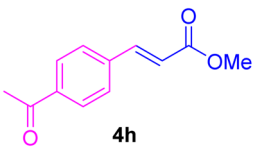 4h	48	80	Trace	NA	NA	—	34–38
11	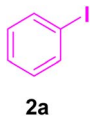 2a	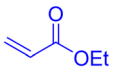 3c	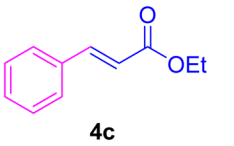 4c	13	80	90	33 330	2564	Liquid	(6.5–7.5) (ref. 138)
12	 2b	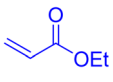 3c	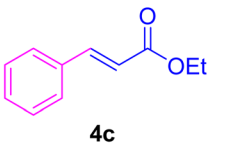 4c	16	80	80	29 630	1852	Liquid	6.5–7.5
13	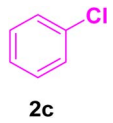 2c	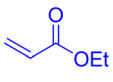 3c	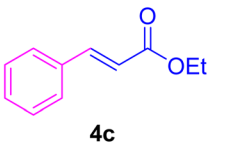 4c	36	80	20	7407	206	Liquid	6.5–7.5
14	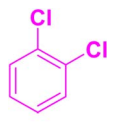 2d	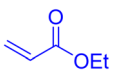 3c	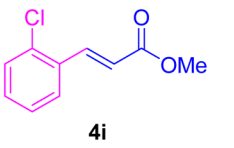 4i	48	80	Trace	NA	NA	—	—
15	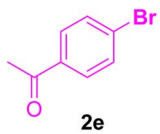 2e	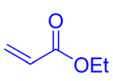 3c	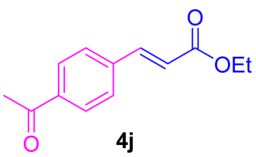 4j	48	80	Trace	NA	NA	—	—
16	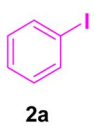 2a	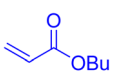 3d	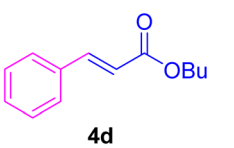 4d	15	80	90	33 330	2222	Liquid[139]	b.p.: 271
17	 2b	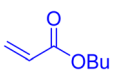 3d	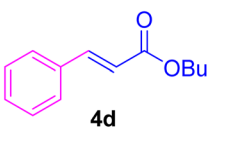 4d	16	80	85	31 481	1968	Liquid	b.p.: 271

Table 2 (*Contd.*)

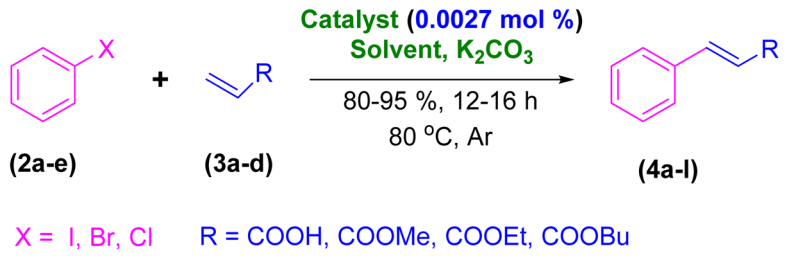

Entry	Ar-X	Alkene	Product	Time (h)	Temp. (°C)	Yield[b] (%)	TON	TOF (h^{-1})	m.p. (°C)	m.p. (°C) (Lit.)
18	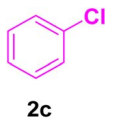 2c	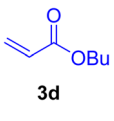 3d	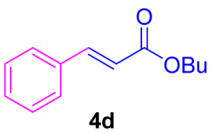 4d	36	80	20	7407	206	Liquid	b.p.: 271
19	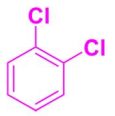 2d	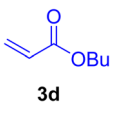 3d	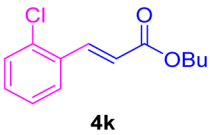 4k	48	80	Trace	NA	NA	—	—
20	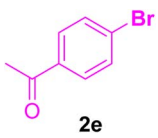 2e	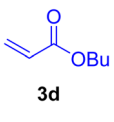 3d	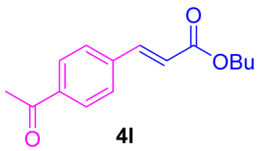 4l	48	80	Trace	NA	NA	—	—

[a] Reaction conditions: aryl halide (**2a–e**, 2.0 mmol), alkene (**3a–d**, 3.0 mmol), K_2CO_3 (2.0 mmol), Pd@MET-EDTA-CS (**1**, 2.0 mg, 0.0027 mol%), and solvent (3.0 mL), under an Ar atmosphere. [b] Isolated yields.

methionine were individually investigated without using any Pd(II) species, but there were no yields of the desired product **4b** obtained (entries 10–15). While the catalyst loading used in the above experiments was just 2.0 mg, other quantities less than 2.0 mg afforded lower reaction yields. Indeed, the utilized catalytic amount was dramatically lower than that in the optimized conditions since the quantity of loaded Pd(II) on the catalyst was just 0.286%. Therefore, the total employed Pd, as an expensive metal, based on the mass of aryl halides was about 0.0027 mol%.

According to the optimization experiments for the model reaction, the impact of various solvents and the amount of the utilized catalyst on the yield of the desired product **4b** is illustrated in Fig. 9. According to the obtained results, as summarized in Table 1 and Fig. 9, the optimized reaction conditions were found to be 2.0 mg catalyst loading (0.0027 mol%) in DMF or CH_3CN solvents at 80–90 °C under an Ar atmosphere.

After the above-mentioned experiments, the scope of the reaction was extended using other aryl halides with electron-withdrawing groups (EWGs) under the optimized conditions. The results are summarized in Table 2. As predicted, by using this novel heterogeneous nanocatalyst, the obtained yields for aryl halides containing EWGs were poor (entries 4, 5, 9, 10, 14, 15, 19 and 20).

3.3. Proposed mechanism for the synthesis of cinnamic acid derivatives in the presence of the catalyst 1 in the HCR

According to the XRD pattern, the oxidation state of the palladium in the Pd@MET-ETDA-CS catalyst (**1**) is (II). Moreover, the active catalytic system in the HCR generally contains Pd(0) species. Therefore, the reduction of Pd(II) in the catalyst **1** to its activated form could be smoothly accomplished in DMF and CH_3CN as oxidizable solvents.[129–131] The proposed mechanism is based on the oxidative addition of the Pd(0) species to the aryl halides **2a–e** to create intermediate **III**, and then a coordination insertion between intermediate **III** and the active alkenes **3a–d** gives intermediate **IV**. Afterward, the migration insertion of hydrogen, followed by C–C bond rotation, generates intermediate **V**, which produces the desired products **4a–l** and intermediate **VI** through the *syn*-β-hydride elimination. Finally, the activated form of the catalyst **1** is recovered by the reductive elimination of HI using K_2CO_3 base (Scheme 2).[132–134]

3.4. Reusability of the Pd@MET-EDTA-CS catalyst (1) in HCR

Reusability of the heterogeneous catalytic systems is one of the main parameters for a specific process. To evaluate this parameter, the model reaction was examined by employing the

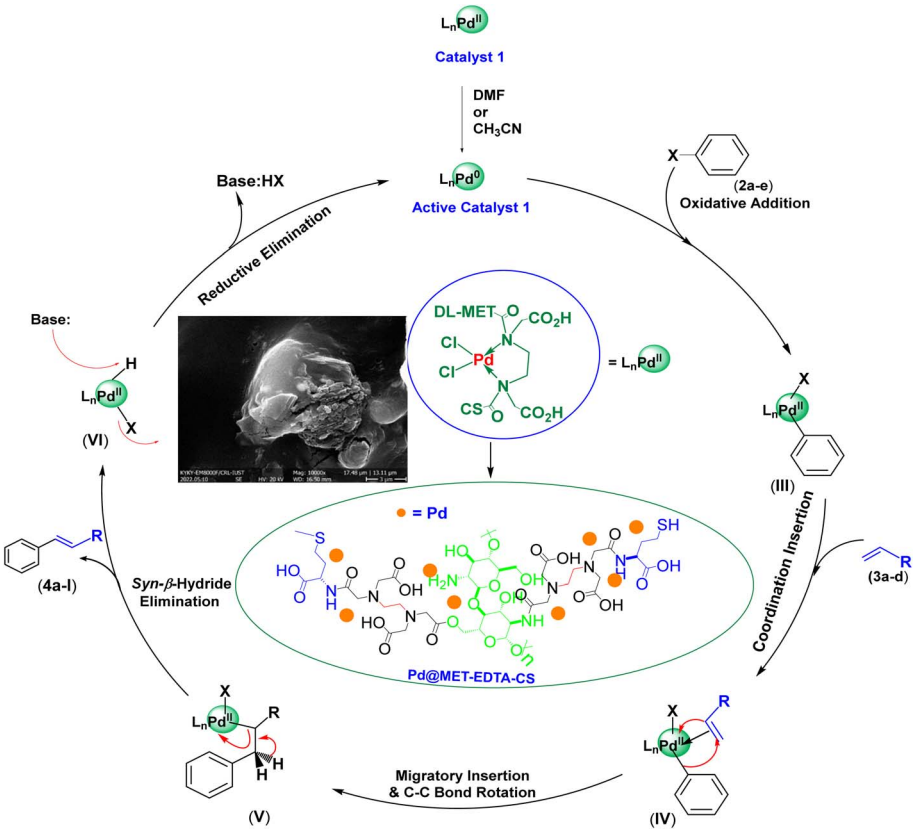

Scheme 2 Proposed mechanism for the synthesis of cinnamic acid derivatives **4** using aryl halides **2** and active alkenes **3** in the presence of the catalyst **1**.

recycled catalyst for five consecutive runs. At the end of each run, the utilized catalyst **1** was removed by a simple filtration and washed with H_2O and EtOH, respectively, followed by drying and reusing in the subsequent model reaction. The obtained results are summarized in Fig. 10. Considering the results of isolated yields for the model reaction, the activity of the catalyst after five cycles remained approximately constant, thus exhibiting a proper conservation of the catalytic activity after its recycling.

3.4.1. FTIR spectra of the fresh and recycled Pd@MET-EDTA-CS catalyst (1). By comparing the both FTIR spectra in Fig. 11, it can be implied that the functional groups in the fresh catalyst **1** stayed the same in the recycled form.

3.4.2. FESEM images for the recycled catalyst 1. FESEM images of the recycled catalyst **1** are illustrated in Fig. 12. As can be seen, the pores and layers of the nanocomposite **1** could be clearly observed, showing the stability of the catalyst after several uses.

3.4.3. XRD patterns of the recycled catalyst 1. The structure of the recycled nanocomposite **1** was also studied by XRD. The obtained pattern for the recycled catalyst was compared with the fresh sample, as shown in Fig. 13. The results demonstrate

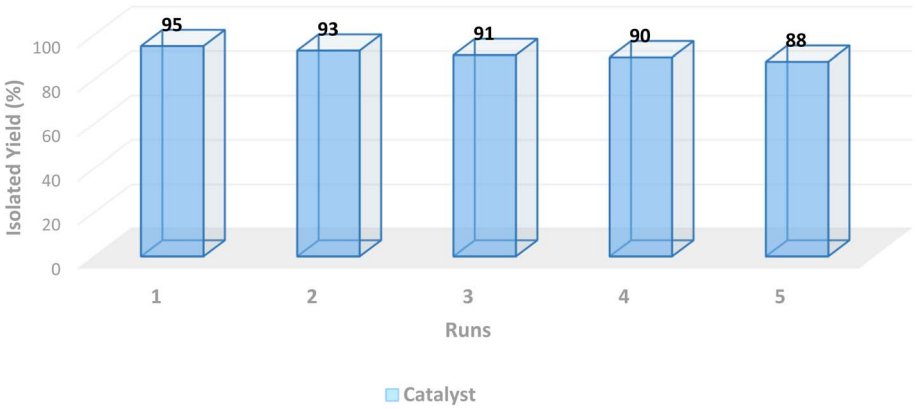

Fig. 10 Reusability of the Pd@MET-EDTA-CS catalyst (**1**) in the model reaction to afford methyl cinnamate (**4b**).

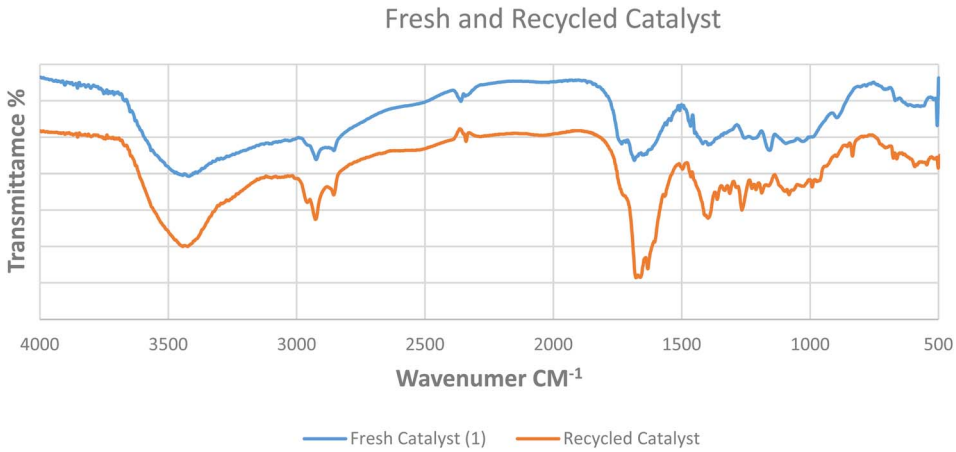

Fig. 11 FTIR of the fresh (blue) and recycled (orange) Pd@MET-EDTA-CS nanocatalyst (**1**).

that the structure of the catalyst **1** was stable during the reaction, even after five runs.

3.5. Leaching test for Pd in the reaction medium (hot filtration test)

Finally, to check the possibility of the leaching of Pd(0) into the reaction medium, the model Heck reaction was heated and stopped after 3 h, and then the catalyst **1** was separated from the hot reaction mixture by filtration. Afterward, the reaction was continued without any catalyst. Although the reaction mixture was heated for about 36 h under the optimized conditions, the progress was stopped at the previous level and the reaction did not proceed more with increasing the time. This expriment demonstrates the heterogeneous nature of the catalyst **1** as no Pd leaching or re-precipitation of the catalyst **1** was observed.

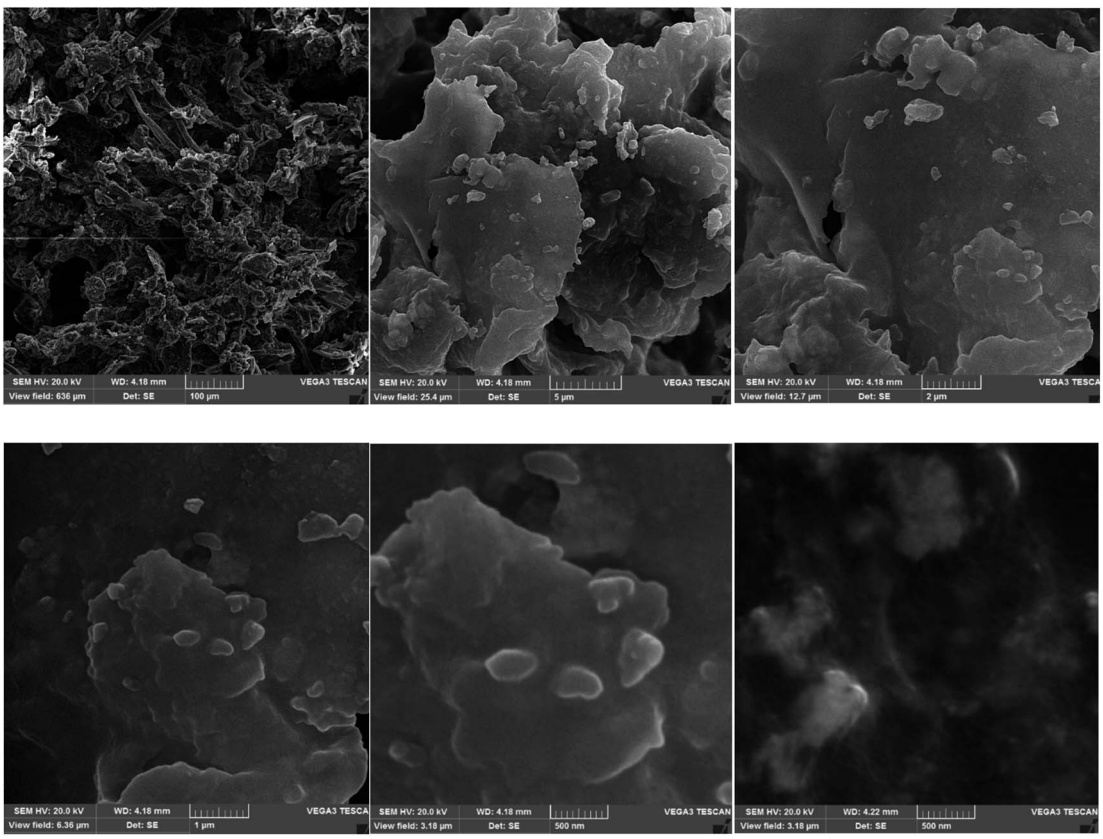

Fig. 12 FESEM images of the recycled nanocatalyst (**1**).

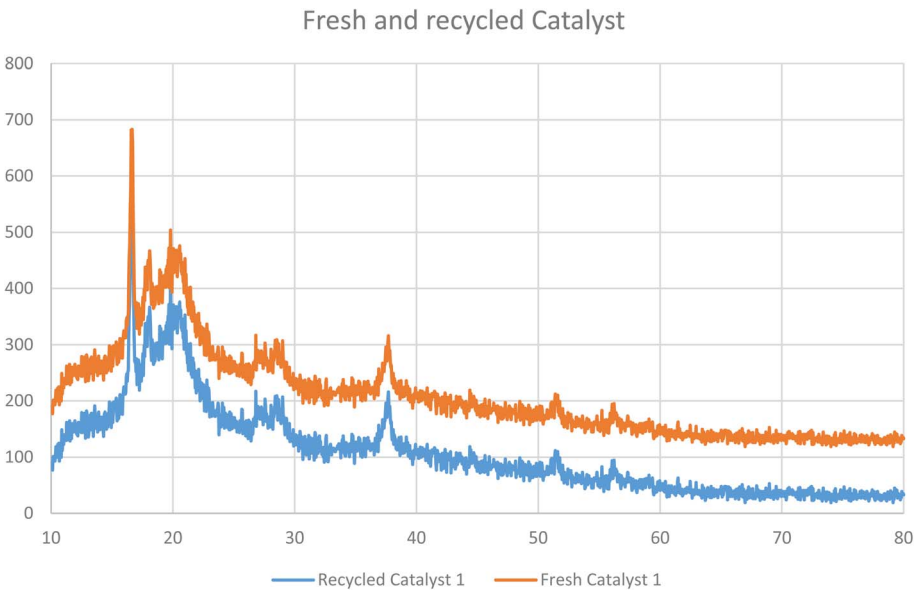

Fig. 13 XRD patterns of the fresh (orange) and recycled (blue) Pd@MET-EDTA-CS nanocatalyst (**1**).

Table 3 Comparison of the obtained results for the HCR using the catalyst **1** and other catalytic systems

Entry	Catalyst	Reaction conditions	Catalyst amount	Time (h)	Yield (%)	Reference
1	Trifunctional *N*,*N*,*O*-terdentate amido/pyridyl carboxylate Pd(II) complexes	DMF/145 °C/Na_2CO_3	0.01 mol%	20	92	140
2	$Pd(OAc)_2$	NMP/135 °C/NaOAc/UV-VIS	0.05 mol%	44	80	141
3	CMH–Pd(0)	DMF/120 °C/Et_3N	50 mg	6	90	142
4	NHC–Pd/IL@SiO_2	NMP/140 °C/NaOAc	0.01 mol%	24	94	143
5	Pd(quinoline-8-carboxylate)$_2$	DMF/130 °C/K_2CO_3	0.01 mol%	30	39–94	144
6	OCMCS–Pd	DMF/140 °C/Et_3N	0.02 mmol	12	89–98	145
7	**Pd@MET-EDTA-CS**	**DMF/90 °C/K_2CO_3**	0.0027 mol%	**16**	**95**	**This work**
8	**Pd@MET-EDTA-CS**	**CH_3CN/80 °C/K_2CO_3**	0.0027 mol%	**18**	**95**	**This work**

3.6. Comparison of the catalytic activity of the Pd@ASP-EDTA-CS catalyst (1) with other catalytic systems

In order to compare the efficacy of the Pd@MET-EDTA-CS catalyst (**1**) with other catalytic systems for application in the HCR, several parameters, including the catalyst loading as well as reaction conditions, required times, and yields of the desired product **4b**, were taken into consideration and the results are summarized in Table 3. It can be seen that the Pd@MET-EDTA-CS heterogeneous catalyst (**1**) showed higher efficiency than the previously reported catalytic systems for the HCR.

4. Conclusions

To conclude, a novel and thermally stable green heterogeneous catalytic system has been prepared by using both naturally abundant chitosan and DL-methionine amino acid, as green resources, grafted by the EDTA linker to produce a natural bio-based support for the chelation of Pd(II) onto the backbone of the modified chitosan. In terms of green metrics, the quantity of the catalyst **1**, compared to other HCRs, was very competitive and cost-effective. On the other hand, the complete recovery of the organic solvents lessened the related impact on the environment. The prepared supramolecular nanocomposite displayed highly efficient catalytic activity, as well as an easy and sustainable application in the HCR to afford the corresponding products in good to excellent yields. The catalyst loading was strongly competitive (0.0027 mol%), which is very interesting due to the high price of Pd sources. The recovery of the catalyst was performed by easy filtration at the end of each run and the catalytic activity stayed approximately constant after five reaction runs without the leaching of Pd species into the reaction medium and the desired products. Therefore, the above-mentioned advantages of the catalyst make it a potential candidate for the pharmaceutical and fine chemical industrial sectors.

Conflicts of interest

There are no conflicts of interest to declare.

Acknowledgements

We are grateful for the financial support from The Research Council of Iran University of Science and Technology (IUST), Tehran, Iran (Grant No 160/22061). We would also like to acknowledge the support of the Iran Nanotechnology Initiative Council (INIC).

References

1 R. F. Heck, Acylation, methylation, and carboxyalkylation of olefins by group VIII metal derivatives, *J. Am. Chem. Soc.*, 1968, **90**(20), 5518–5526.
2 N. Miyaura, K. Yamada and A. Suzuki, A new stereospecific cross-coupling by the palladium-catalyzed reaction of 1-alkenylboranes with 1-alkenyl or 1-alkynyl halides, *Tetrahedron Lett.*, 1979, **20**(36), 3437–3440.
3 K. Sonogashira, Y. Tohda and N. Hagihara, A convenient synthesis of acetylenes: catalytic substitutions of acetylenic hydrogen with bromoalkenes, iodoarenes and bromopyridines, *Tetrahedron Lett.*, 1975, **16**(50), 4467–4470.
4 A. O. King, N. Okukado and E.-I. Negishi, Highly general stereo-, regio-, and chemo-selective synthesis of terminal and internal conjugated enynes by the Pd-catalysed reaction of alkynylzinc reagents with alkenyl halides, *J. Chem. Soc., Chem. Commun.*, 1977, **19**, 683–684.
5 K. Tamao, K. Sumitani and M. Kumada, Selective carbon-carbon bond formation by cross-coupling of Grignard reagents with organic halides. Catalysis by nickel-phosphine complexes, *J. Am. Chem. Soc.*, 1972, **94**(12), 4374–4376.
6 D. Milstein and J. Stille, A general, selective, and facile method for ketone synthesis from acid chlorides and organotin compounds catalyzed by palladium, *J. Am. Chem. Soc.*, 1978, **100**(11), 3636–3638.
7 B. M. Trost and T. J. Fullerton, New synthetic reactions. Allylic alkylation, *J. Am. Chem. Soc.*, 1973, **95**(1), 292–294.
8 J. Magano and J. R. Dunetz, Recent large-scale applications of transition metal-catalyzed couplings for the synthesis of pharmaceuticals, in *New Trends in Cross-Coupling*, 2014, pp. 697–778.
9 C. Torborg and M. Beller, Recent applications of palladium-catalyzed coupling reactions in the pharmaceutical, agrochemical, and fine chemical industries, *Adv. Synth. Catal.*, 2009, **351**(18), 3027–3043.
10 T. Mizoroki, K. Mori and A. Ozaki, Arylation of olefin with aryl iodide catalyzed by palladium, *Bull. Chem. Soc. Jpn.*, 1971, **44**(2), 581.
11 R. F. Heck and J. Nolley Jr, Palladium-catalyzed vinylic hydrogen substitution reactions with aryl, benzyl, and styryl halides, *J. Org. Chem.*, 1972, **37**(14), 2320–2322.
12 J. Terao, H. Watanabe, A. Ikumi, H. Kuniyasu and N. Kambe, Nickel-Catalyzed Cross-Coupling Reaction of Grignard Reagents with Alkyl Halides and Tosylates: remarkable Effect of 1,3-Butadienes, *J. Am. Chem. Soc.*, 2002, **124**(16), 4222–4223.
13 T. M. Gøgsig, J. Kleimark, S. O. Nilsson Lill, S. Korsager, A. T. Lindhardt, P.-O. Norrby and T. Skrydstrup, Mild and Efficient Nickel-Catalyzed Heck Reactions with Electron-Rich Olefins, *J. Am. Chem. Soc.*, 2012, **134**(1), 443–452.
14 N. Paul, T. Patra and D. Maiti, Recent Developments in Hydrodecyanation and Declarative Functionalization Reactions, *Asian J. Org. Chem.*, 2022, **11**(1), e202100591.
15 K. Juhász, Á. Magyar and Z. Hell, Transition-Metal-Catalyzed Cross-Coupling Reactions of Grignard Reagents, *Synthesis*, 2021, **53**(6), 983–1002.
16 S. Chandra, A. Roy, M. Jana and K. Pahan, Cinnamic acid activates PPARα to stimulate Lysosomal biogenesis and lower Amyloid plaque pathology in an Alzheimer's disease mouse model, *Neurobiol. Dis.*, 2019, **124**, 379–395.
17 O. M. Abd El-Raouf, E. S. M. El-Sayed and M. F. Manie, Cinnamic acid and cinnamaldehyde ameliorate cisplatin-induced splenotoxicity in rats, *J. Biochem. Mol. Toxicol.*, 2015, **29**(9), 426–431.
18 G. D. D. A. Lima, M. P. Rodrigues, T. A. D. O. Mendes, G. A. Moreira, R. P. Siqueira, A. M. da Silva, B. G. Vaz, J. L. R. Fietto, G. C. Bressan, M. Machado-Neves and R. R. Teixeira, Synthesis and antimetastatic activity evaluation of cinnamic acid derivatives containing 1,2,3-triazole portions, *Toxicol. in Vitro*, 2018, **53**, 1–9.
19 R. Wang, W. Yang, Y. Fan, W. Dehaen, Y. Li, H. Li, W. Wang, Q. Zheng and Q. Huai, Design and synthesis of the novel oleanolic acid-cinnamic acid ester derivatives and glycyrrhetinic acid-cinnamic acid ester derivatives with cytotoxic properties, *Bioorg. Chem.*, 2019, **88**, 102951.
20 J. M. Gießel, A. Loesche, S. Hoenke and R. Csuk, In search of new cinnamic acid derived flavours and fragrances, *Results Chem.*, 2019, **1**, 100010.
21 J.-S. Lan, J.-W. Hou, Y. Liu, Y. Ding, Y. Zhang, L. Li and T. Zhang, Design, synthesis and evaluation of novel cinnamic acid derivatives bearing *N*-benzyl pyridinium moiety as multifunctional cholinesterase inhibitors for Alzheimer's disease, *J. Enzyme Inhib. Med. Chem.*, 2017, **32**(1), 776–788.
22 S. Guo, Y. Zhen, Z. Zhu, G. Zhou and X. Zheng, Cinnamic acid rescues behavioral deficits in a mouse model of traumatic brain injury by targeting miR-455-3p/HDAC2, *Life Sci.*, 2019, **235**, 116819.
23 S. Adisakwattana, J. Pongsuwan, C. Wungcharoen and S. Yibchok-anun, In vitro effects of cinnamic acid derivatives on protein tyrosine phosphatase 1B, *J. Enzyme Inhib. Med. Chem.*, 2013, **28**(5), 1067–1072.
24 A. Gunia-Krzyzak and E. Zesławska, Cinnamic acid derivatives in cosmetics: current use and future prospects, *Int. J. Cosmet. Sci.*, 2018, **40**, 356–366.
25 S. Prateek, Cinnamic acid derivatives: a new chapter of various pharmacological activities, *J. Chem. Pharm. Res.*, 2011, **3**(2), 403–423.
26 C. Letizia, J. Cocchiara, A. Lapczynski, J. Lalko and A. Api, Fragrance material review on cinnamic acid, *Food Chem. Toxicol.*, 2005, **43**(6), 925–943.

27 G. V. Ambulgekar, B. M. Bhanage and S. D. Samant, Low temperature recyclable catalyst for Heck reactions using ultrasound, *Tetrahedron Lett.*, 2005, **46**(14), 2483–2485.
28 W. H. Perkin, XI.—On the formation of coumarin and of cinnamic and of other analogous acids from the aromatic aldehydes, *J. Chem. Soc.*, 1877, **31**, 388–427.
29 M. Gupta and B. P. Wakhloo, Tetrabutylammoniumbromide mediated Knoevenagel condensation in water: synthesis of cinnamic acids, *Arkivoc*, 2007, **2007**, 94–98.
30 A. Mobinikhaledi, N. Foroughifar and H. F. Jirandehi, Microwave-assisted synthesis of cinnamic acid derivatives in the presence of PPE and under solvent-free condition, *Synth. React. Inorg., Met.-Org., Nano-Met. Chem.*, 2008, **38**(5), 428–430.
31 A. Avanesyan, A. Simonyan and M. Simonyan, Phosphorus Oxychloride in Organic Synthesis. Part 3: synthesis of α-Benzoylaminocinnamic Acids, *Pharm. Chem. J.*, 2005, **39**(7), 379–380.
32 B. P. Joshi, A. Sharma and A. K. Sinha, Efficient one-pot, two-step synthesis of (*E*)-cinnamaldehyde by dehydrogenation–oxidation of arylpropanes using DDQ under ultrasonic irradiation, *Tetrahedron*, 2006, **62**(11), 2590–2593.
33 M.-F. Tsai, S.-M. Huang, H.-Y. Huang, S.-W. Tsai, C.-H. Kuo and C.-J. Shieh, Ultrasound Plus Vacuum-System-Assisted Biocatalytic Synthesis of Octyl Cinnamate and Response Surface Methodology Optimization, *Molecules*, 2022, **27**(21), 7148.
34 G.-S. Lee, A. Widjaja and Y.-H. Ju, Enzymatic synthesis of cinnamic acid derivatives, *Biotechnol. Lett.*, 2006, **28**(8), 581–585.
35 R.-X. Liang and Y.-X. Jia, Aromatic π-Components for Enantioselective Heck Reactions and Heck/Anion-Capture Domino Sequences, *Acc. Chem. Res.*, 2022, **55**(5), 734–745.
36 M. Dohendou, K. Pakzad, Z. Nezafat, M. Nasrollahzadeh and M. G. Dekamin, Progresses in chitin, chitosan, starch, cellulose, pectin, alginate, gelatin and gum based (nano)catalysts for the Heck coupling reactions: a review, *Int. J. Biol. Macromol.*, 2021, **192**, 771–819.
37 S. S. Ray and M. Bousmina, Biodegradable polymers and their layered silicate nanocomposites: in greening the 21st century materials world, *Prog. Mater. Sci.*, 2005, **50**(8), 962–1079.
38 J. K. Pandey, A. P. Kumar, M. Misra, A. K. Mohanty, L. T. Drzal and R. Palsingh, Recent advances in biodegradable nanocomposites, *J. Nanosci. Nanotechnol.*, 2005, **5**(4), 497–526.
39 M. Madrahalli Bharamanagowda and R. K. Panchangam, Fe_3O_4-Lignin@ Pd-NPs: a highly efficient, magnetically recoverable and recyclable catalyst for Mizoroki–Heck reaction under solvent-free conditions, *Appl. Organomet. Chem.*, 2020, **34**(10), e5837.
40 H. Wang, F. Wang, X. Li, Q. Xiao, W. Luo and J. Xu, In situ formation of electron-deficient Pd sites on AuPd alloy nanoparticles under irradiation enabled efficient photocatalytic Heck reaction, *Chin. J. Catal.*, 2023, **46**, 72–83.
41 H. Keypour, J. Kouhdareh, S. Alavinia, K. Rabiei, M. Mohammadi, A. Maryamabadi and S. Babaei, Post-synthetic modification of dual-porous UMCM-1-NH_2 with palladacycle complex as an effective heterogeneous catalyst in Suzuki and Heck coupling reactions, *J. Organomet. Chem.*, 2023, **989**, 122646.
42 Y. Rangraz, F. Nemati and A. Elhampour, Organoselenium–palladium(ii) complex immobilized on functionalized magnetic nanoparticles as a promising retrievable nanocatalyst for the "phosphine-free" Heck–Mizoroki coupling reaction, *New J. Chem.*, 2018, **42**(18), 15361–15371.
43 D. N. Fodor, T. S. Kégl, J. Z. M. Tukacs, A. K. Horváth and L. S. T. Mika, Homogeneous Pd-catalyzed Heck coupling in γ-valerolactone as a green reaction medium: a catalytic, kinetic, and computational study, *ACS Sustainable Chem. Eng.*, 2020, **8**(26), 9926–9936.
44 C. C. Cassol, A. P. Umpierre, G. Machado, S. I. Wolke and J. Dupont, The role of Pd nanoparticles in ionic liquid in the Heck reaction, *J. Am. Chem. Soc.*, 2005, **127**(10), 3298–3299.
45 S. R. Attar and S. B. Kamble, Recent advances in nanoparticles towards sustainability and their application in organic transformations in aqueous media, *Nanoscale*, 2022, **14**(45), 16761–16786.
46 J. Guerra and M. A. Herrero, Hybrid materials based on Pd nanoparticles on carbon nanostructures for environmentally benign C–C coupling chemistry, *Nanoscale*, 2010, **2**(8), 1390–1400.
47 N. Norouzi, M. K. Das, A. J. Richard, A. A. Ibrahim, H. M. El-Kaderi and M. S. El-Shall, Heterogeneous catalysis by ultra-small bimetallic nanoparticles surpassing homogeneous catalysis for carbon–carbon bond forming reactions, *Nanoscale*, 2020, **12**(37), 19191–19202.
48 Y. Yang, C. E. Castano, B. F. Gupton, A. C. Reber and S. N. Khanna, A fundamental analysis of enhanced cross-coupling catalytic activity for palladium clusters on graphene supports, *Nanoscale*, 2016, **8**(47), 19564–19572.
49 M. Opanasenko, P. Štěpnička and J. Čejka, Heterogeneous Pd catalysts supported on silica matrices, *RSC Adv.*, 2014, **4**(110), 65137–65162.
50 A. Kamal, V. Srinivasulu, B. N. Seshadri, N. Markandeya, A. Alarifi and N. Shankaraiah, Water mediated Heck and Ullmann couplings by supported palladium nanoparticles: importance of surface polarity of the carbon spheres, *Green Chem.*, 2012, **14**(9), 2513–2522.
51 S. Sobhani, H. Hosseini Moghadam, J. Skibsted and J. M. Sansano, A hydrophilic heterogeneous cobalt catalyst for fluoride-free Hiyama, Suzuki, Heck and Hirao cross-coupling reactions in water, *Green Chem.*, 2020, **22**(4), 1353–1365.
52 Z. Shahamat, F. Nemati and A. Elhampour, Palladium(II) anchored on a magnetic mesoporous polymelamine–formaldehyde as new catalyst for Heck coupling reaction: optimization of reaction using response surface methodology, *J. Porous Mater.*, 2020, **27**, 107–122.

53 S. Sadjadi, M. M. Heravi and M. Raja, Composite of ionic liquid decorated cyclodextrin nanosponge, graphene oxide and chitosan: a novel catalyst support, *Int. J. Biol. Macromol.*, 2019, **122**, 228–237.

54 Y. Bao, L. Shao, G. Xing and C. Qi, Cobalt, nickel and iron embedded chitosan microparticles as efficient and reusable catalysts for Heck cross-coupling reactions, *Int. J. Biol. Macromol.*, 2019, **130**, 203–212.

55 M. B. Marulasiddeshwara and P. R. Kumar, Synthesis of Pd(0) nanocatalyst using lignin in water for the Mizoroki–Heck reaction under solvent-free conditions, *Int. J. Biol. Macromol.*, 2016, **83**, 326–334.

56 M. Zeng, X. Yuan, Z. Yang and C. Qi, Novel macroporous palladium cation crosslinked chitosan membranes for heterogeneous catalysis application, *Int. J. Biol. Macromol.*, 2014, **68**, 189–197.

57 M. Nasrollahzadeh, N. S. S. Bidgoli, Z. Issaabadi, Z. Ghavamifar, T. Baran, R. Luque and L. Hibiscus Rosasinensis, aqueous extract-assisted valorization of lignin: preparation of magnetically reusable Pd NPs@Fe_3O_4-lignin for Cr(VI) reduction and Suzuki–Miyaura reaction in eco-friendly media, *Int. J. Biol. Macromol.*, 2020, **148**, 265–275.

58 N. Shaikh and P. Pamidimukkala, Magnetic chitosan stabilized palladium nanostructures: potential catalysts for aqueous Suzuki coupling reactions, *Int. J. Biol. Macromol.*, 2021, **183**, 1560–1573.

59 G. Wang, K. Lv, T. Chen, Z. Chen and J. Hu, Immobilizing of palladium on melamine functionalized magnetic chitosan beads: a versatile catalyst for p-nitrophenol reduction and Suzuki reaction in aqueous medium, *Int. J. Biol. Macromol.*, 2021, **184**, 358–368.

60 M. Çalışkan and T. Baran, Decorated palladium nanoparticles on chitosan/δ-FeOOH microspheres: a highly active and recyclable catalyst for Suzuki coupling reaction and cyanation of aryl halides, *Int. J. Biol. Macromol.*, 2021, **174**, 120–133.

61 H. Joshi, K. N. Sharma, A. K. Sharma and A. K. Singh, Palladium–phosphorus/sulfur nanoparticles (NPs) decorated on graphene oxide: synthesis using the same precursor for NPs and catalytic applications in Suzuki–Miyaura coupling, *Nanoscale*, 2014, **6**(9), 4588–4597.

62 G. Albano, A. Petri and L. A. Aronica, Palladium Supported on Bioinspired Materials as Catalysts for C–C Coupling Reactions, *Catalysts*, 2023, **13**(1), 210.

63 S. Hasanzadeh Banakar, M. G. Dekamin and A. Yaghoubi, Selective and highly efficient synthesis of xanthenedione or tetraketone derivatives catalyzed by ZnO nanorod-decorated graphene oxide, *New J. Chem.*, 2018, **42**(17), 14246–14262.

64 K. Hong, M. Sajjadi, J. M. Suh, K. Zhang, M. Nasrollahzadeh, H. W. Jang, R. S. Varma and M. Shokouhimehr, Palladium nanoparticles on assorted nanostructured supports: applications for Suzuki, Heck, and Sonogashira cross-coupling reactions, *ACS Appl. Nano Mater.*, 2020, **3**(3), 2070–2103.

65 F. Christoffel and T. R. Ward, Palladium-Catalyzed Heck Cross-Coupling Reactions in Water: a Comprehensive Review, *Catal. Lett.*, 2018, **148**(2), 489–511.

66 M. Nasrollahzadeh, Z. Issaabadi, M. M. Tohidi and S. Mohammad Sajadi, Recent progress in application of graphene supported metal nanoparticles in C–C and C–X coupling reactions, *Chem. Rec.*, 2018, **18**(2), 165–229.

67 G. S. Lee, D. Kim and S. H. Hong, Pd-catalyzed formal Mizoroki–Heck coupling of unactivated alkyl chlorides, *Nat. Commun.*, 2021, **12**(1), 991.

68 K. Hasan, C. Fowler, P. Kwong, A. K. Crane, J. L. Collins and C. M. Kozak, Synthesis and structure of iron(III) diamine-bis(phenolate) complexes, *Dalton Trans.*, 2008, (22), 2991–2998.

69 T. Baran and M. Nasrollahzadeh, Facile synthesis of palladium nanoparticles immobilized on magnetic biodegradable microcapsules used as effective and recyclable catalyst in Suzuki–Miyaura reaction and p-nitrophenol reduction, *Carbohydr. Polym.*, 2019, **222**, 115029.

70 M. G. Dekamin, S. Ilkhanizadeh, Z. Latifidoost, H. Daemi, Z. Karimi and M. Barikani, Alginic acid: a highly efficient renewable and heterogeneous biopolymeric catalyst for one-pot synthesis of the Hantzsch 1,4-dihydropyridines, *RSC Adv.*, 2014, **4**(100), 56658–56664.

71 N. Sharma, H. Ojha, A. Bharadwaj, D. P. Pathak and R. K. Sharma, Preparation and catalytic applications of nanomaterials: a review, *RSC Adv.*, 2015, **5**(66), 53381–53403.

72 M. Zeng, C. Qi and X.-M. Zhang, Chitosan microspheres supported palladium heterogeneous catalysts modified with pearl shell powders, *Int. J. Biol. Macromol.*, 2013, **55**, 240–245.

73 M. Zeng, X. Zhang, C. Qi and X.-M. Zhang, Microstructure-stability relations studies of porous chitosan microspheres supported palladium catalysts, *Int. J. Biol. Macromol.*, 2012, **51**(5), 730–737.

74 S. Ilkhanizadeh, J. Khalafy and M. G. Dekamin, Sodium alginate: a biopolymeric catalyst for the synthesis of novel and known polysubstituted pyrano[3,2-*c*]chromenes, *Int. J. Biol. Macromol.*, 2019, **140**, 605–613.

75 S. Nikolov, M. Petrov, L. Lymperakis, M. Friák, C. Sachs, H. O. Fabritius, D. Raabe and J. Neugebauer, Revealing the design principles of high-performance biological composites using *ab initio* and multiscale simulations: the example of lobster cuticle, *Adv. Mater.*, 2010, **22**(4), 519–526.

76 T. Baran, I. Sargin, M. Kaya and A. Menteş, Green heterogeneous Pd (II) catalyst produced from chitosan-cellulose micro beads for green synthesis of biaryls, *Carbohydr. Polym.*, 2016, **152**, 181–188.

77 M. G. Dekamin, M. Azimoshan and L. Ramezani, Chitosan: a highly efficient renewable and recoverable bio-polymer catalyst for the expeditious synthesis of α-amino nitriles and imines under mild conditions, *Green Chem.*, 2013, **15**(3), 811–820.

78 Z. Alirezvani, M. G. Dekamin and E. Valiey, Cu (II) and magnetite nanoparticles decorated melamine-functionalized chitosan: a synergistic multifunctional catalyst for sustainable cascade oxidation of benzyl alcohols/Knoevenagel condensation, *Sci. Rep.*, 2019, **9**(1), 17758.

79 M. G. Dekamin, E. Kazemi, Z. Karimi, M. Mohammadalipoor and M. R. Naimi-Jamal, Chitosan: an efficient biomacromolecule support for synergic catalyzing of Hantzsch esters by $CuSO_4$, *Int. J. Biol. Macromol.*, 2016, **93**, 767–774.

80 N. Rostami, M. Dekamin, E. Valiey and H. Fanimoghadam, Chitosan-EDTA-Cellulose network as a green, recyclable and multifunctional biopolymeric organocatalyst for the one-pot synthesis of 2-amino-4*H*-pyran derivatives, *Sci. Rep.*, 2022, **12**(1), 8642.

81 W. Wang, C. Xue and X. Mao, Chitosan: structural modification, biological activity and application, *Int. J. Biol. Macromol.*, 2020, **164**, 4532–4546.

82 E. Valiey, M. G. Dekamin and Z. Alirezvani, Melamine-modified chitosan materials: an efficient and recyclable bifunctional organocatalyst for green synthesis of densely functionalized bioactive dihydropyrano[2,3-*c*]pyrazole and benzylpyrazolyl coumarin derivatives, *Int. J. Biol. Macromol.*, 2019, **129**, 407–421.

83 M. G. Dekamin, Z. Karimi, Z. Latifidoost, S. Ilkhanizadeh, H. Daemi, M. R. Naimi-Jamal and M. Barikani, Alginic acid: a mild and renewable bifunctional heterogeneous biopolymeric organocatalyst for efficient and facile synthesis of polyhydroquinolines, *Int. J. Biol. Macromol.*, 2018, **108**, 1273–1280.

84 N. Rostami, M. G. Dekamin and E. Valiey, Chitosan-EDTA-Cellulose bio-based network: a recyclable multifunctional organocatalyst for green and expeditious synthesis of Hantzsch esters, *Carbohydr. Polym. Technol. Appl.*, 2023, **5**, 100279.

85 M. G. Dekamin, S. Z. Peyman, Z. Karimi, S. Javanshir, M. R. Naimi-Jamal and M. Barikani, Sodium alginate: an efficient biopolymeric catalyst for green synthesis of 2-amino-4*H*-pyran derivatives, *Int. J. Biol. Macromol.*, 2016, **87**, 172–179.

86 W. Luo, K. Luo, Y. Yang, X. Lin, P. Li and Y. Wen, *N*-maleyl chitosan-supported palladium catalyst for Heck coupling reaction and reduction of 4-nitrophenol, *Colloids Surf., A*, 2022, **652**, 129852.

87 M. Çalışkan and T. Baran, Nanoscaled reusable palladium catalyst supported on chitosan hybrid composite microcapsules reinforced with ZnO nanoparticles for Heck coupling reactions, *Cellulose*, 2022, **29**(14), 7789–7802.

88 H. D. Güzel, M. Çalışkan and T. Baran, Supported Pd nanoparticles on micro structured chitosan-MgAl layered double hydroxide hydrogel beads as a sustainable, effective, and recyclable nanocatalyst for Heck cross-coupling reactions, *J. Phys. Chem. Solids*, 2022, **167**, 110777.

89 M. W. TM, W. M. Lau and V. V. Khutoryanskiy, Chitosan and Its Derivatives for Application in Mucoadhesive Drug Delivery Systems, *Polymers*, 2018, **10**(3), 267.

90 G. J. Dee, O. Rhode and R. Wachter, Chitosan: multi-functional marine polymer, *Cosmet. Toiletries*, 2001, **116**(2), 39–44.

91 Z. Alirezvani, M. G. Dekamin, F. Davoodi and E. Valiey, Melamine-Functionalized Chitosan: a New Bio-Based Reusable Bifunctional Organocatalyst for the Synthesis of Cyanocinnamonitrile Intermediates and Densely Functionalized Nicotinonitrile Derivatives, *ChemistrySelect*, 2018, **3**(37), 10450–10463.

92 A. S. SM Sadiri and M. G. Dekamin, Amperometric glucose sensor based on nickel nanoparticle/chitosan and multiwall carbon nanotube on modified graphite electrode, *Am. J. Anal. Chem.*, 2014, **6**, 173–178.

93 I. Issahaku, I. K. Tetteh and A. Y. Tetteh, Chitosan and chitosan derivatives: recent advancements in production and applications in environmental remediation, *Environ. Adv.*, 2023, **11**, 100351.

94 L. Z. Nikoshvili, B. B. Tikhonov, P. E. Ivanov, P. Y. Stadolnikova, M. G. Sulman and V. G. Matveeva, Recent Progress in Chitosan-Containing Composite Materials for Sustainable Approaches to Adsorption and Catalysis, *Catalysts*, 2023, **13**(2), 367.

95 L. A. Picos-Corrales, A. M. Morales-Burgos, J. P. Ruelas-Leyva, G. Crini, E. García-Armenta, S. A. Jimenez-Lam, L. E. Ayón-Reyna, F. Rocha-Alonzo, L. Calderón-Zamora, U. Osuna-Martínez, A. Calderón-Castro, G. De-Paz-Arroyo and L. N. Inzunza-Camacho, Chitosan as an Outstanding Polysaccharide Improving Health-Commodities of Humans and Environmental Protection, *Polymers*, 2023, **15**(3), 526.

96 I. Fusteş-Dămoc, T. Măluţan and A. Mija, Chitosan as a Polyfunctional Crosslinker for a Renewable-Based Resorcinol Diglycidyl Ether, *ACS Sustainable Chem. Eng.*, 2023, **11**(19), 7605–7616.

97 C. Kaliaperumal and A. Thulasisingh, Electrospun polycaprolactone/chitosan/pectin composite nanofibre: a novel wound dressing scaffold, *Bull. Mater. Sci.*, 2023, **46**(1), 23.

98 J. Rathod, P. Sharma, P. Pandey, A. Singh and P. Kumar, Highly active recyclable SBA-15-EDTA-Pd catalyst for Mizoroki–Heck, Stille and Kumada C–C coupling reactions, *J. Porous Mater.*, 2017, **24**(4), 837–846.

99 M. Chtchigrovsky, A. Primo, P. Gonzalez, K. Molvinger, M. Robitzer, F. Quignard and F. Taran, Functionalized chitosan as a green, recyclable, biopolymer-supported catalyst for the [3 + 2] Huisgen cycloaddition, *Angew. Chem., Int. Ed.*, 2009, **48**(32), 5916–5920.

100 H. Honarkar and M. Barikani, Applications of biopolymers I: chitosan, *Monatsh. fur Chem.*, 2009, **140**(12), 1403–1420.

101 K. Landfester, Miniemulsion polymerization and the structure of polymer and hybrid nanoparticles, *Angew. Chem., Int. Ed.*, 2009, **48**(25), 4488–4507.

102 Y. Wang, F. Wang, L. Shu, P. Wu, Z. Li, J. Gao and H. Liu, Novel Sustainable Adsorbents Prepared by Banana/

Pomegranate Peels *via* EDTA Grafting for Effective Removal of Cd(II), Co(II), Mn(II), and Ni(II) from Sewage System, *Water, Air, Soil Pollut.*, 2023, **234**(2), 131.

103 R. Daneshfar, M. Karimi Nouroddin, S. Z. Mousavi Golsefid, M. Mohammadi-Khanaposhtani, E. Davoudi and K. Shariati, Experimental Investigation and Modeling of Fluid and Carbonated Rock Interactions with EDTA Chelating Agent during EOR Process, *Energy Fuels*, 2023, **37**(2), 919–934.

104 M. Ostovar, A. Ghasemi, F. Karimi, N. Saberi and B. Vriens, Assessment of EDTA-enhanced electrokinetic removal of metal(loid)s from phosphate mine tailings, *Sep. Sci. Technol.*, 2023, **58**(3), 613–625.

105 D. Naghipour, J. Jaafari, S. D. Ashrafi and A. H. Mahvi, Remediation of heavy metals contaminated silty clay loam soil by column extraction with ethylenediaminetetraacetic acid and nitrilo triacetic acid, *J. Environ. Eng.*, 2017, **143**(8), 04017026.

106 F. Zhao, E. Repo, D. Yin, L. Chen, S. Kalliola, J. Tang, E. Iakovleva, K. C. Tam and M. Sillanpää, One-pot synthesis of trifunctional chitosan-EDTA-β-cyclodextrin polymer for simultaneous removal of metals and organic micropollutants, *Sci. Rep.*, 2017, **7**(1), 15811.

107 K. Khomthawee, N. Nilada, A. Homchuen and P. Saejueng, Chitosan-EDTA-palladium composite for the Suzuki–Miyaura reaction, *Appl. Organomet. Chem.*, 2022, e6987.

108 E. Valiey, M. G. Dekamin and S. Bondarian, Sulfamic acid grafted to cross-linked chitosan by dendritic units: a bio-based, highly efficient and heterogeneous organocatalyst for green synthesis of 2,3-dihydroquinazoline derivatives, *RSC Adv.*, 2023, **13**(1), 320–334.

109 P. G. de Abrantes, I. F. Costa, N. K. D. S. M. Falcão, J. M. G. de Oliveira Ferreira, C. G. L. Junior, E. E. D. S. Teotonio and J. A. Vale, The Efficient Knoevenagel Condensation Promoted by Bifunctional Heterogenized Catalyst Based Chitosan-EDTA at Room Temperature, *Catal. Lett.*, 2022, (153), 945–955.

110 N. Rostami, M. G. Dekamin, E. Valiey and H. FaniMoghadam, l-asparagine–EDTA–amide silica-coated MNPs: a highly efficient and nano-ordered multifunctional core–shell organocatalyst for green synthesis of 3,4-dihydropyrimidin-2 (1*H*)-one compounds, *RSC Adv.*, 2022, **12**(34), 21742–21759.

111 E. Valiey and M. G. Dekamin, Supported copper on a diamide–diacid-bridged PMO: an efficient hybrid catalyst for the cascade oxidation of benzyl alcohols/Knoevenagel condensation, *RSC Adv.*, 2022, **12**(1), 437–450.

112 M. Dohendou, M. G. Dekamin and D. Namaki, Pd@l-asparagine-EDTA-chitosan: a highly effective and reusable bio-based and biodegradable catalyst for the Heck cross-coupling reaction under mild conditions, *Nanoscale Adv.*, 2023, **5**(9), 2621–2638.

113 F. Zuo, Q. Gu, S. Li, H. Wei and J. Peng, Effects of Different Methionine Sources on Methionine Metabolism in the IPEC-J2 Cells, *BioMed Res. Int.*, 2019, **2019**, 5464906.

114 C. Bunchasak, Role of dietary methionine in poultry production, *Poult. Sci. J.*, 2009, **46**(3), 169–179.

115 D. Vyas and R. Erdman, Meta-analysis of milk protein yield responses to lysine and methionine supplementation, *J. Dairy Sci.*, 2009, **92**(10), 5011–5018.

116 I. Mavromichalis, D. M. Webel, J. L. Emmert, R. L. Moser and D. H. Baker, Limiting order of amino acids in a low-protein corn-soybean meal-whey-based diet for nursery pigs, *J. Anim. Sci.*, 1998, **76**(11), 2833–2837.

117 National Center for Biotechnology Information, PubChem Compound Summary for CID 6137, Methionine, 2022, **https://pubchem.ncbi.nlm.nih.gov/compound/Methionine.2022**.

118 M. Nasrollahzadeh, S. M. Sajadi, A. Rostami-Vartooni and A. Azarian, Palladium nanoparticles supported on copper oxide as an efficient and recyclable catalyst for carbon (sp^2)–carbon (sp^2) cross-coupling reaction, *Mater. Res. Bull.*, 2015, **68**, 150–154.

119 M. A. Zolfigol, T. Azadbakht, V. Khakyzadeh, R. Nejatyami and D. M. Perrin, C (sp^2)–C (sp^2) cross coupling reactions catalyzed by an active and highly stable magnetically separable Pd-nanocatalyst in aqueous media, *RSC Adv.*, 2014, **4**(75), 40036–40042.

120 A. Ghorbani-Choghamarani, B. Tahmasbi and P. Moradi, Synthesis of a new Pd(0)-complex supported on boehmite nanoparticles and study of its catalytic activity for Suzuki and Heck reactions in H_2O or PEG, *RSC Adv.*, 2016, **6**(49), 43205–43216.

121 A. R. Hajipour, Z. Khorsandi and H. Farrokhpour, Regioselective Heck reaction catalyzed by Pd nanoparticles immobilized on DNA-modified MWCNTs, *RSC Adv.*, 2016, **6**(64), 59124–59130.

122 S. Sheikh, M. A. Nasseri, M. Chahkandi, O. Reiser and A. Allahresani, Dendritic structured palladium complexes: magnetically retrievable, highly efficient heterogeneous nanocatalyst for Suzuki and Heck cross-coupling reactions, *RSC Adv.*, 2022, **12**(15), 8833–8840.

123 M. A. Gotthardt, A. Beilmann, R. Schoch, J. Engelke and W. Kleist, Post-synthetic immobilization of palladium complexes on metal–organic frameworks – a new concept for the design of heterogeneous catalysts for Heck reactions, *RSC Adv.*, 2013, **3**(27), 10676–10679.

124 S. Fujita and N. Sakairi, Water soluble EDTA-linked chitosan as a zwitterionic flocculant for pH sensitive removal of Cu(II) ion, *RSC Adv.*, 2016, **6**(13), 10385–10392.

125 N. Arsalani and S. Z. Mousavi, Synthesis and characterization of water-soluble and carboxy-functional polyester and polyamide based on ethylenediamine-tetraacetic acid and their metal complexes, *Iran. Polym. J.*, 2003, **12**(4), 291–296.

126 N. Rostami, M. G. Dekamin, E. Valiey and H. Fanimoghadam, Chitosan-EDTA-Cellulose network as a green, recyclable and multifunctional biopolymeric organocatalyst for the one-pot synthesis of 2-amino-4*H*-pyran derivatives, *Sci. Rep.*, 2022, **12**(1), 8642.

127 J. J. Verendel, T. L. Church and P. G. Andersson, Catalytic One-Pot Production of Small Organics from Polysaccharides, *Synthesis*, 2011, **2011**(11), 1649–1677.

128 S. Kumar and J. Koh, Physiochemical, Optical and Biological Activity of Chitosan-Chromone Derivative for Biomedical Applications, *Int. J. Mol. Sci.*, 2012, 6102–6116.
129 J. Sherwood, J. H. Clark, I. J. Fairlamb and J. M. Slattery, Solvent effects in palladium catalysed cross-coupling reactions, *Green Chem.*, 2019, **21**(9), 2164–2213.
130 A. Jutand, Dual role of nucleophiles in palladium-catalyzed Heck, Stille, and Sonogashira reactions, *Pure Appl. Chem.*, 2004, **76**(3), 565–576.
131 J. A. Molina de la Torre, P. Espinet and A. C. Albeniz, Solvent-induced reduction of palladium-aryls, a potential interference in Pd catalysis, *Organometallics*, 2013, **32**(19), 5428–5434.
132 A. Carral-Menoyo, N. Sotomayor and E. Lete, Palladium-catalysed Heck-type alkenylation reactions in the synthesis of quinolines. Mechanistic insights and recent applications, *Catal. Sci. Technol.*, 2020, **10**(16), 5345–5361.
133 F. Jafarpour, N. Jalalimanesh, M. Teimouri and M. Shamsianpour, Palladium/norbornene chemistry: an unexpected route to methanocarbazole derivatives *via* three C sp^3–C sp^2/C sp^3–N/C sp^2–N bond formations in a single synthetic sequence, *Chem. Commun.*, 2015, **51**(1), 225–228.
134 A. M. Alazemi, K. M. Dawood, H. M. Al-Matar and W. M. Tohamy, Efficient and Recyclable Solid-Supported Pd(II) Catalyst for Microwave-Assisted Suzuki Cross-Coupling in Aqueous Medium, *ACS Omega*, 2022, **7**(33), 28831–28848.
135 **https://www.guidechem.com/encyclopedia/trans-cinnamic-acid-dic3044.html**, *trans*-Cinnamic acid.
136 **https://www.hzchempro.com/product/116868-96-3.html** (*E*)-3-(4-acetylphenyl)acrylic acid.
137 **https://www.guidechem.com/dictionary/en/1896-62-4.html**, *trans*-4-Phenyl-3-buten-2-one. pp **https://www.guidechem.com/dictionary/en/1896-62-4.html**.
138 **https://www.guidechem.com/encyclopedia/ethyl-cinnamate-dic1774.html**, Ethyl cinnamate.
139 S. Bhatia, G. Wellington, J. Cocchiara, J. Lalko, C. Letizia and A. Api, Fragrance material review on butyl cinnamate, *Food Chem. Toxicol.*, 2007, **45**(1), S49–S52.
140 M. L. Kantam, P. Srinivas, J. Yadav, P. R. Likhar and S. Bhargava, Trifunctional *N*,*N*,*O*-terdentate amido/pyridyl carboxylate ligated Pd(II) complexes for Heck and Suzuki reactions, *J. Org. Chem.*, 2009, **74**(13), 4882–4885.
141 M. A. Fredricks, M. Drees and K. Köhler, Acceleration of the rate of the heck reaction through UV-and visible-light-induced palladium (II) reduction, *ChemCatChem*, 2010, **2**(11), 1467–1476.
142 C. Wu, X. Peng, L. Zhong, X. Li and R. Sun, Green synthesis of palladium nanoparticles *via* branched polymers: a bio-based nanocomposite for C–C coupling reactions, *RSC Adv.*, 2016, **6**(38), 32202–32211.
143 B. Karimi and D. Enders, New N-heterocyclic carbene palladium complex/ionic liquid matrix immobilized on silica: application as recoverable catalyst for the Heck reaction, *Org. Lett.*, 2006, **8**(6), 1237–1240.
144 X. Cui, J. Li, Z.-P. Zhang, Y. Fu, L. Liu and Q.-X. Guo, Pd (quinoline-8-carboxylate) 2 as a low-priced, phosphine-free catalyst for Heck and Suzuki reactions, *J. Org. Chem.*, 2007, **72**(24), 9342–9345.
145 D. Lv and M. Zhang, *O*-carboxymethyl chitosan supported heterogeneous palladium and Ni catalysts for heck reaction, *Molecules*, 2017, **22**(1), 150.